

Active control of flow-induced cavity oscillations

Louis N. Cattafesta III^{a,*}, Qi Song^a, David R. Williams^b, Clarence W. Rowley^c, Farrukh S. Alvi^d

^a Mechanical and Aerospace Engineering, University of Florida, P.O. Box 116250, Gainesville, FL 32611-6250, USA

^b MMAE Department, Illinois Institute of Technology, E-1 Bldg., 3110 S. State St., Chicago, IL 60616, USA

^c Mechanical and Aerospace Engineering, Princeton University, D232 E-quad, Princeton, NJ 08544, USA

^d Mechanical Engineering, Florida A&M and Florida State University, 2525 Pottsdamer St., Tallahassee, FL 32310, USA

ARTICLE INFO

Available online 11 September 2008

Keywords:

Active flow control
Cavity oscillations
Cavity resonance
Flow-induced oscillations
Actuators
Feedback control

ABSTRACT

A review of active control of flow-induced cavity oscillations is motivated by two factors. First, the search for solutions to the practical problem of suppressing oscillations caused by flow over open cavities has generated significant interest in this area. Second, cavity oscillation control serves as a model problem in the growing multidisciplinary field of flow control. As such, we attempt to summarize recent activities in this area, with emphasis on experimental implementation of open- and closed-loop control approaches. In addition to describing successes, failures, and outstanding issues relevant to cavity oscillations, we highlight the characteristics of the various actuators, flow sensing and measurement, and control methodologies employed to date in order to emphasize the choices, challenges, and potential of flow control in this and other applications, such as impact on store trajectory.

© 2008 Elsevier Ltd. All rights reserved.

Contents

1. Introduction	479
2. Suppression of cavity oscillations	481
2.1. Flow-control classifications	481
2.2. Passive/active and open-loop suppression studies	482
2.3. Effect of control on the flow field and store trajectory	487
3. Sensors and actuators	488
3.1. Passive actuators	488
3.2. Active open-loop actuators	489
3.3. Active closed-loop actuators	490
3.4. Sensors and flow measurements	493
4. Closed-loop control methodologies	493
4.1. Quasi-static vs. dynamic controllers	496
4.2. Models	496
4.2.1. System identification	496
4.2.2. POD/Galerkin models	497
4.2.3. Rossiter-type models	497
4.3. Control algorithms	497
4.3.1. State estimation: observers and static estimators	499
4.4. Fundamental limits on achievable performance	499
5. Summary and outlook	500
Acknowledgements	500
References	500

1. Introduction

Flow over cavities has received a great deal of interest over the last several years because of practical and academic interests

* Corresponding author. Tel.: +1352 846 3017; fax: +1352 392 7303.
E-mail address: cattafes@ufl.edu (L.N. Cattafesta III).

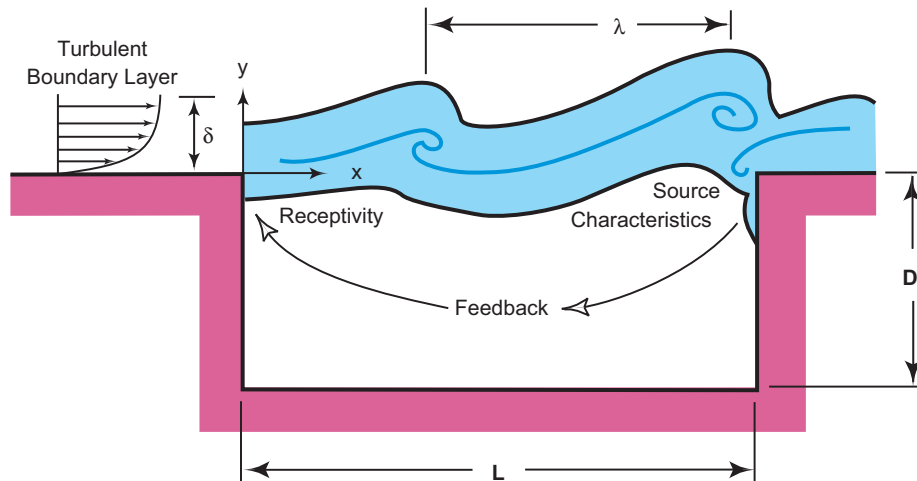


Fig. 1. Schematic illustrating flow-induced cavity resonance for an upstream turbulent boundary layer.

associated with controlling such flows. The problem of accurate prediction and control over a wide range of flow conditions is not solved. The need to accurately model the disparate scales of acoustic and vortical disturbances driving the oscillations is a difficult task for fluid dynamicists and aeroacousticians, while control theorists are challenged by the multiple competing modes of oscillation that must be controlled to achieve suppression. These and a number of other issues have established flow-induced cavity oscillations as a canonical problem in flow control.

The nature of flow-induced oscillations in an open cavity is illustrated in Fig. 1. A boundary layer of thickness δ and momentum thickness θ separates at the upstream edge of the cavity of length L , depth D , and width W . The resulting shear layer develops based on its initial conditions (imposed by the upstream boundary layer and cavity acoustic field) and the instability characteristics of the mean shear-layer profile. The shear layer spans the length of the cavity and ultimately reattaches near the trailing edge of the cavity in an “open” cavity flow. The reattachment region acts as the primary acoustic source. Acoustic waves travel inside the cavity (and outside for subsonic flow), towards the cavity leading edge. The incident acoustic waves force the shear layer, setting the initial amplitude and phase of the instability waves through a receptivity process. These instabilities grow to form large-scale vortical structures that convect downstream at a fraction of the free stream speed before impinging near the trailing edge.

The overall process produces resonant frequencies, which are referred to as *cavity tones*. Fig. 2 illustrates representative, unsteady pressure spectra (dB re 20 μ Pa) at Mach 2 for a range of cavity length/depth L/D ratios [1]. The spectra are dominated by high-amplitude, discrete-frequency tones and large broadband levels. In many cases, multiple tones are observed, and these are often accompanied by their harmonics. In the context of cavity flows, the flow–acoustic coupling which leads to resonance is commonly called the *Rossiter mechanism* [2], although a similar phenomenological model was proposed for the edge-tone problem more than a decade earlier by Powell [3]. The relevant dimensionless parameters are L/D , L/W , and L/θ , as well as the flow parameters p_{rms}/q_∞ , Reynolds number Re_θ , Mach number M_∞ , and shape factor $H = \delta^*/\theta$, where p_{rms} is the rms pressure fluctuation, q_∞ is the free stream dynamic pressure, and δ^* and θ are the displacement and momentum thicknesses, respectively, of the upstream boundary layer.

Cavity flows have been the subject of numerous studies since the 1950s [4,5], and we do not attempt to provide a comprehen-

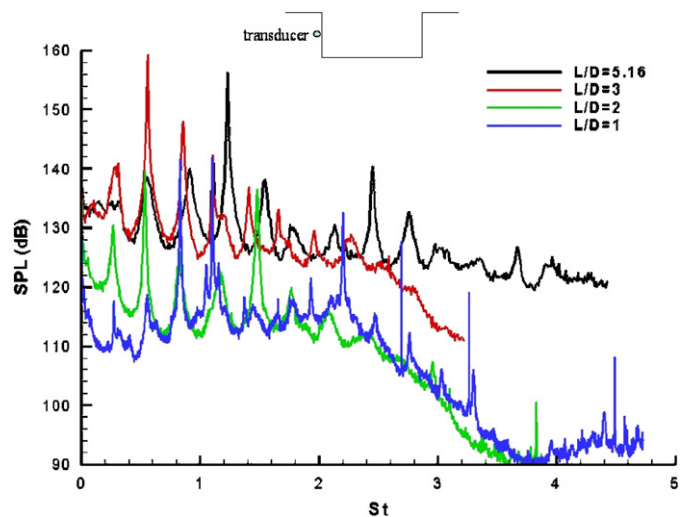


Fig. 2. Pressure spectra for different L/D cavities at $M_\infty = 2$. Unsteady pressure spectra measured using a transducer located at the upstream wall, as shown in the inset (from Zhuang et al. [1]). The dimensionless frequency is the Strouhal number $St = fL/U_\infty$.

sive review of the subject here. The interested reader is referred to several reviews spanning three decades of research [6–14]. In particular, the review by Colonius [12] provides a summary of numerical simulations and flow-physics modeling, permitting us to largely ignore these relevant topics.

Control of grazing flow over cavities is pertinent to a wide range of real-world applications, ranging from landing-gear and weapons bays in aircraft to flow in gas transport systems [15], over sunroofs and windows in automobiles [16], and in instrument or telescope bays [17]. The high dynamic loads illustrated in Fig. 2 are generally present in all of these applications and can lead to structural fatigue of the cavity and its contents or, in the case of compressible flow, aero-optic distortion [18]. In addition, the highly oscillatory flow field generated by cavity flows can adversely affect the safe departure and accurate delivery of munitions stored in the weapons bay. This problem has become more acute with the recent emphasis on store separation of “smart” weapons that are lighter and more compact [19].

Although the overall goal of control is usually to reduce the flow unsteadiness in some form, the specific objective of what

constitutes “*effective control*” is largely dependent on the application. In strongly resonant cases, where one or more discrete tones are dominant compared to the background broadband level, attenuation of the tones is generally sufficient. However, in situations where the broadband levels may be comparable to the tonal amplitudes, a reduction in the overall (integrated) noise levels may be required. In still other applications, such as aero-optics, the objective may be to reduce optical wavefront aberrations caused by flow-induced, index-of-refraction variations. In any case, the key is to translate the application objective to an effective flow-control strategy and, in the case of closed-loop control, to a mathematical statement of the control objective.

Therefore, the primary purpose of this review is to summarize recent activities in active control of flow-induced cavity oscillations, with particular emphasis on implementation of open- and closed-loop control approaches. In addition to describing successes, failures, and outstanding issues relevant to cavity oscillations, we highlight the characteristics of various actuators, flow sensing and measurement, and control methodologies in order to emphasize the choices, challenges, and potential of flow control.

The paper is organized as follows. Section 2 provides a brief overview of passive and open-loop suppression studies and discusses the application to store separation. While recent studies are emphasized, some classical studies are reviewed to place these new results in proper context. Section 3 describes actuators and flow measurements, while closed-loop control and pertinent

modeling/design approaches are summarized in Section 4. Finally, Section 5 provides a summary and offers our perspective on outstanding issues and future directions.

2. Suppression of cavity oscillations

2.1. Flow-control classifications

Techniques to suppress cavity oscillations can be classified in several ways. In this paper, we choose the classification shown in Fig. 3, to be consistent with the terminology used in active noise and vibration control. Active control provides *external* energy (e.g., mechanical or electrical) input to an adjustable actuator to control the flow, while passive control techniques do not. Passive control of cavity oscillations has been successfully implemented via geometric modifications using, for example, fixed fences, spoilers, ramps [20,21], and a passive bleed system [22]. Note that some control devices considered passive by this classification extract energy from the flow itself and have been called “*active*” by other researchers. Pertinent examples include unpowered or passive resonance tubes [19,23] and cylinders or rods placed in the boundary layer near the leading edge of the cavity [24,25]. These devices, described further in Section 3, are sometimes referred to as active because they provide an oscillatory input to the flow, but their effect on the flow cannot be adjusted without either changing the flow conditions or changing the device itself.

Active control is further divided into open- and closed-loop approaches. As shown in Fig. 4, by its very definition, closed-loop control implies a feedback loop, in which some flow quantity is directly sensed or estimated and fed back to modify the control signal [26]. Open loop corresponds to the case when there is no feedback loop.

A further non-standard but useful classification of closed-loop flow control is that of quasi-static vs. dynamic feedback control. The quasi-static case corresponds to slow tuning of an open-loop control approach and occurs when the time scales of feedback are large compared to the time scales of the plant (i.e., flow). This approach is particularly relevant in nonlinear fluid dynamic systems, where the fundamental notion of frequency preservation in a linear system does not hold. As discussed in Section 5, the quasi-static approach was successfully used by Shaw and

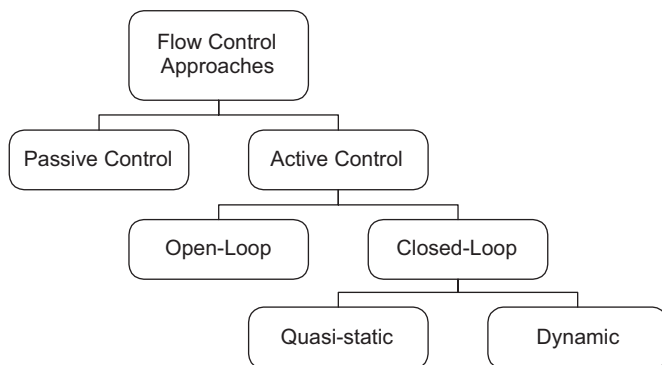


Fig. 3. Possible classification of flow-control approaches.

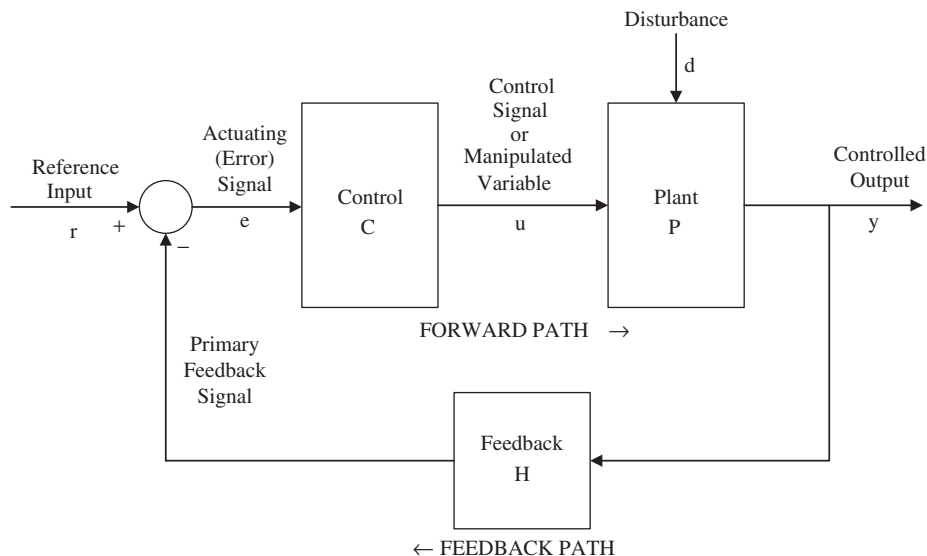


Fig. 4. Components of a feedback control system [26]. The various time-domain signals are in lower case, while the transfer functions of the blocks are in upper case (Laplace domain).

Northcraft [27]. The usual dynamic compensation case corresponds to the situation when the above time scales are commensurate. This can be implemented using an analog (see, for example, Williams et al. [28]) or “real-time” digital control systems [29]. In this context, “real time” refers to the situation in which the control signal is updated at the sampling rate of the data system, and the actuator response to the flow state changes at the time scales of the dynamics.

2.2. Passive/active and open-loop suppression studies

Table 1 provides a detailed list of passive/active and open-loop cavity suppression studies. Where possible, the cavity dimensions and flow conditions are summarized. The methods and key results are also included. The investigations are listed in chronological order for historical purposes. It is impossible to include all prior research; there are numerous other (mostly passive) studies that have not been included here because most of these have been summarized in the other reviews cited earlier. Some key observations are discussed here.

Sarohia and Massier [30] studied the efficacy of *steady* mass injection at the base or floor of two different axisymmetric cavity models for both laminar and turbulent boundary layers. While base injection was effective at suppressing cavity tones, large mass flow rates were required— $B_c = 5\text{--}15\%$. The mass flow rate parameter used by the authors is equivalent to that proposed later by Vakili and Gauthier [31] for rectangular cavities:

$$B_c = \left(\frac{\rho_w V_w}{\rho_e V_e} \right) \frac{A_{inj}}{A_{cavity}} = \frac{\dot{m}}{\rho_e V_e A_{cavity}}, \quad (1)$$

where A_{inj} is the total injector area, and $A_{cavity} = LW$ is the area of the cavity exposed to the free stream flow.

Sarno and Franke [32] studied static and oscillating fences, and also steady and pulsed injection (at 0° or 45° with respect to the free stream direction) at transonic speeds near the cavity leading edge. Blowing coefficients B_c of up to 7% were used. While the static fences provided the best suppression, the bandwidth of the mechanical fences was limited to $<220\text{ Hz}$, while the pulsed injection was $<80\text{ Hz}$. These frequencies were at least an order-of-magnitude lower than the frequencies of the cavity tones, and thereby constituted a quasi-static or low-frequency forcing. Nonetheless, they represented an important step in the evolution of active control of cavity oscillations, both in terms of approach and also the introduction of scaling laws for such actuators.

Vakili and Gauthier [31] obtained significant acoustic tone attenuation with steady normal mass injection through variable-density porous plates upstream of the cavity leading edge at Mach 1.8 using $B_c \sim 4\%$. They attributed the attenuation to a thickening of the cavity shear layer and a corresponding alteration of its instability characteristics.

McGrath and Shaw [24] subsequently studied mechanical oscillations of hinged flaps at frequencies up to 35 Hz over a range of subsonic and supersonic Mach numbers. Similar to the Sarno and Franke experiments, the forcing frequency was an order-of-magnitude lower than the resonant tone frequency. The static and oscillatory deflections were on the order of the boundary layer thickness δ and were shown to be effective despite their limited bandwidth.

McGrath and Shaw were the first to study the effect of a cylinder placed in the upstream subsonic boundary layer. Because of the well-known shedding characteristics of a circular cylinder of diameter d , $St = fd/U \approx 0.2$, over a wide Reynolds number range, this device was called a high-frequency tone generator (HFTG). The cylinder was capable of producing substantial reductions of both the cavity tones and the broadband. The authors attributed

the potential mechanism of the actuator to the interaction of the shed vortices with the shear-layer instabilities. As will be discussed later, however, there are additional possible mechanisms noted by other investigators that influence the suppression effectiveness of the cylinder.

At the same time in the mid-1990s, Ahuja and his colleagues were investigating other novel control strategies. For example, Mendoza and Ahuja [33] studied the effect of a steady wall jet on the tone production mechanism, using a Coanda surface. Although no mass flow measurements were obtained, upstream boundary layer profiles showed an increase in δ with blowing, thereby leading to the hypothesis that the suppression was due to reduced amplification of the shear-layer instabilities.

Hsu and Ahuja [34] studied the effect of a trailing-edge array of Helmholtz resonators (i.e., commercial syringes) on cavity noise, and they obtained some suppression at lower Mach numbers. At intermediate Mach numbers, the resonators reduced the magnitude of the targeted tone, but new tones appeared at other frequencies—a phenomenon that has been observed by many researchers. At high Mach numbers, no suppression was obtained, but the authors believed that the reason was likely due to the difficulty in setting the small resonator volume accurately. This study is noteworthy for its attempt to control cavity oscillations in the vicinity of the acoustic source origin near the trailing-edge impingement region. Generally, actuators are placed at the leading edge of the cavity to leverage the growth of instabilities in the shear layer.

In 1997, Cattafesta et al. [35] presented the use of a six-element piezoelectric flap array flush mounted at the leading edge of the cavity. The bandwidth of the actuators was large enough ($\sim 300\text{ Hz}$) to provide forcing at frequencies comparable to that of the cavity tones. Open-loop sinusoidal forcing at a sufficient amplitude and appropriate detuned frequency was capable of suppressing the cavity tone. Shear-layer velocity measurements indicated that the actuators seeded the shear layer with a disturbance that was large enough to prevent the growth of the natural cavity disturbances. However, the possibility of starving the growth of natural instabilities at high subsonic and supersonic Mach numbers is questionable, because of the large amount of mean-flow energy available ($\sim M_\infty^2$) for disturbance amplification.

In 1998, Shaw continued his study of leading-edge HFTGs, low-frequency pulsed-fluidic injection, and oscillating flaps [36]. While various diameter HFTGs mounted at a fixed height were shown to be effective, the suppression improved as the diameter was increased. However, the relative height of the cylinder in the boundary layer was not reported, which is now known to be an important parameter. Shaw also discussed two potential mechanisms of the HFTG: (1) high-frequency forcing due to shedding and (2) reduced shear-layer growth rates due to boundary layer thickening.

Rescaling Shaw's pulsed-blowing results shows that they are consistent with prior results, since B_c values of a few percent were required to suppress the tones. However, no spectra were reported to assess the impact of blowing on the broadband noise. Interestingly, the tone amplitude continued to decrease as the pulse frequency of the injector reached its upper limit of 100 Hz. Furthermore, normal injection was shown to be superior to tangential blowing.

The oscillatory flap frequency in Shaw's experiment was varied from 0 to 100 Hz and provided maximum suppression at 5 Hz. A monotonic improvement (reduction) in unsteady pressure level occurred as the dynamic deflection angle increased to its upper limit, corresponding to a deflection of order δ . However, the increase in δ for a full-scale aircraft led Shaw to conclude that this approach (low-frequency, large-amplitude, open-loop forcing) was not feasible for a full-scale aircraft.

Table 1
Summary of selected passive and active and open-loop cavity suppression studies

Study	Conditions	Method	Comments
Sarohia and Massier [30]	<ul style="list-style-type: none"> Two axisymmetric cavity models $L/D = 0-1.5$ $M_\infty = 0-0.5$ Laminar and turbulent BL 	<ul style="list-style-type: none"> Steady injection at base of the cavity $B_c \sim 5-15\%$ 	<ul style="list-style-type: none"> Large mass flow rates were required to stabilize cavity oscillations
Sarno and Franke [32]	<ul style="list-style-type: none"> $L/D = 2, L/W = 6.4$ at $M_\infty = 0.6, 0.7, 0.9, 1.1, 1.3, 1.5$ Calculated $\delta = 0.048$ in (at $M_\infty = 1.53$) to 0.062 in (at $M_\infty = 0.62$) 	<ul style="list-style-type: none"> Static and oscillating mechanical fences (< 220 Hz) Steady and pulsed flow injection (< 80 Hz) at either 0° or 45° w.r.t. free stream at leading edge B_c up to 7% 	<ul style="list-style-type: none"> Insufficient actuator bandwidth Low-frequency forcing ineffective Significant 3-D effects possible
Vakili and Gauthier [31]	<ul style="list-style-type: none"> $L/D = L/W = 2.54, M_\infty = 1.8$ $Re_\delta = 3.68 \times 10^5$ 	<ul style="list-style-type: none"> Obtained significant attenuation with steady mass injection through porous plates upstream of cavity leading edge $B_c \sim 4\%$ 	<ul style="list-style-type: none"> Proposed blowing coefficient $B_c = \frac{\left(\frac{\rho_w V_w}{\rho_e V_e}\right) \frac{A_{inj}}{A_{cavity}}}{\rho_\infty U_\infty A_{cavity}} = \frac{\dot{m}}{\rho_\infty U_\infty A_{cavity}}$ <ul style="list-style-type: none"> Attenuation attributed to thickening of cavity shear layer to alter its instability characteristics
McGrath and Shaw [24]	<ul style="list-style-type: none"> $L/D = 2.56, 3.73, 6.83$ $Re/m = 6.6 \times 10^6$ $\delta = 0.13$ in at $M_\infty = 0.85$ 	<ul style="list-style-type: none"> Mechanical oscillations of hinged flap up to 35 Hz at $M_\infty = 0.6, 0.8, 1.5, 1.89$ Static and oscillatory deflections of up to 1δ Cylinder ($d = 0.062$ in) placed in upstream cavity BL at $M_\infty = 0.6, 0.8 \rightarrow$ called high-frequency tone generator HFTG Based on shedding concept $St = fd/U = 0.2$ for $Re_d = 10^3-10^5$ 	<ul style="list-style-type: none"> Oscillating flaps show effective reduction of tones at subsonic and supersonic flow conditions Limited bandwidth of actuator HFTG shows effective reduction of tones and broadband Proposed mechanism is the interaction of shed vortices with shear-layer instabilities Resonance effects?
Mendoza and Ahuja [33]	<ul style="list-style-type: none"> $L/D = 3.75, L/W = 0.47$ $M_\infty = 0.36, 0.44, 0.55, 0.9, 1.05$ $\delta = 0.057, 0.059, 0.062$ in at $M_\infty = 0.36, 0.44, 0.55$, respectively 	<ul style="list-style-type: none"> Studied effects of steady wall jet on cavity noise (normal via 0.2 mm slot and upstream via a 1/4 in radius of curvature Coanda surface 0.5625 in upstream of cavity leading edge) Proposed $\delta/L > 0.07$ for elimination of cavity tones 	<ul style="list-style-type: none"> Upstream BL profiles showed an increase in δ with upstream blowing from Coanda surface Hypothesized that suppression is due to reduced shear-layer growth rate No injected mass flow measurements provided
Hsu and Ahuja [34]	<ul style="list-style-type: none"> $L/D = 2.5, L/W = 0.47$ $M_\infty = 0.34, 0.53, 0.9$ 	<ul style="list-style-type: none"> Studied effect of trailing-edge array of Helmholtz resonators (commercial syringes) on cavity noise 	<ul style="list-style-type: none"> No effect of resonators when in their closed position Significant reductions observed at low Mach numbers, but new tones can appear Negligible suppression at $M = 0.9$ Reason may be due to difficulty in accurately setting correct volume of all resonators
Cattafesta et al. [35]	<ul style="list-style-type: none"> $L/D = 0.5, L/W = 0.5, U_\infty = 40$ m/s, $Re_\theta = 4750, L/\theta = 81$ $L/D = 2.0, L/W = 2.0, U_\infty = 45$ m/s, $Re_\theta = 5210, L/\theta = 328$ 	<ul style="list-style-type: none"> Used piezoelectric flaps flush mounted at the leading edge of the cavity to suppress low-speed cavity oscillations 	<ul style="list-style-type: none"> OL forcing at detuned frequency suppresses oscillations Shear-layer meas. w/ & w/o control. Also CL results
Lamp and Chokani [38]	<ul style="list-style-type: none"> $L/D = 4, L/W = 3$ $M_\infty = 0.15, 0.23$ $Re/m = 5.9 \times 10^6$ 	<ul style="list-style-type: none"> Used rotary valve actuator to provide steady and/or oscillatory blowing 0.1 in upstream of cavity at frequencies up to 750 Hz Used $\langle c_\mu \rangle = \rho u_{rms}^2 A_j / q A_r$ up to 0.16% where $A_r =$ cavity front wall area (2 by 1.5 in) up to 0.16% 	<ul style="list-style-type: none"> Configuration emphasized 3-D effects Showed that oscillatory blowing can reduce tone amplitude significantly (up to 10 dB) provided frequency of forcing is not a harmonic of the cavity resonance, but new tones appear at the forcing frequency

Table 1 (continued)

Study	Conditions	Method	Comments
Shaw [36]	<ul style="list-style-type: none"> • $L/D = \sim 6.5$, $L/W = 3.67$ • $M_\infty = 0.6, 0.85, 0.95, 1.05$ • $\delta \sim 0.38$ in • $Re/m = 6.6 \times 10^6$ 	<ul style="list-style-type: none"> • Studied leading edge oscillating flaps, pulsed fluidic actuation, and HFTG using 1/16, 1/8, and 3/16 in diameter cylindrical rods located at a height of 0.3 in 	<ul style="list-style-type: none"> • Discussed possible mechanisms of HFTG (mode competition, shear-layer instability) • Low-freq. notched flaps effective when oscillating flap reaches BL edge • Showed normal injection ($B_c < 4.5\%$) superior to tangential
Fabris and Williams [37]	<ul style="list-style-type: none"> • $L/D = 4$, $L/W = 0.49$ • $M_\infty = 0.15, 0.23$ ($\theta = 3.1$ mm) 	<ul style="list-style-type: none"> • Unsteady bleed forcing (second mode) through a 12.7 mm slot located 12.7 mm ahead of cavity leading edge via speakers 	<ul style="list-style-type: none"> • Shear-layer receptive to unsteady bleed forcing
Raman et al. [39,40]	<ul style="list-style-type: none"> • $L/D = 6$, $L/W = 1.7$ • $M_\infty = 0.4-0.7$ • Jet cavity configuration 	<ul style="list-style-type: none"> • Used upstream miniature fluidic oscillators to suppress cavity oscillations via sine, square, and triangular waveforms up to 3 kHz with mass flow rates of only 0.12% of main jet flow 	<ul style="list-style-type: none"> • Comparable steady injection and upstream acoustic excitation do not suppress the cavity resonance • Hypothesized that periodic sweeping motion in spanwise direction destroys the spanwise coherence of shear layer
Stanek et al. [19]	<ul style="list-style-type: none"> • $L/D = L/W = 5$ • $M_\infty = 0.4, 0.6, 0.85, 0.95, 1.19, 1.35$ • Calculated $\delta = 10.5$ mm @ $M_\infty = 0.6$, $Re/m = 11 \times 10^6$ 	<ul style="list-style-type: none"> • Investigated “high-frequency” powered resonance tubes, protruding piezoceramic driven wedges, a cylindrical rod, and passive resonance tubes vs. conventional “low-frequency” 1 δ spoiler 	<ul style="list-style-type: none"> • Successful hifex forcing for powered resonance tube at $B_c = 1.6\%$ • Hypothesize that mechanism is “accelerated energy cascade”
Bueno et al. [48]	<ul style="list-style-type: none"> • $M_\infty = 2$, $\delta = 0.53$ in • $Re/m = 3.0 \times 10^7$ • $L/D = 5, 6, 8, 9$, $W/D = 3$ 	<ul style="list-style-type: none"> • Six fast-response (~ 3 ms) jets used to study effects of upstream pulsed and steady mass injection via a staggered configuration • Studied single short duration (1–2 ms) and long duration (50% duty cycle of forcing frequency of 50 or 80 Hz) pulses 	<ul style="list-style-type: none"> • $B_c = 0.28\%, 0.24\%, 0.18\%, 0.16\%$ at $L/D = 5, 6, 8, 9$, respectively, for continuous injection with all six valves • Found that continuous mass injection was more effective than pulsed injection in suppressing tones and overall noise level
Ukeiley et al. [25]	<ul style="list-style-type: none"> • At $M_\infty = 0.6, 0.75$, $\delta = 0.1, 0.08$ in, $Re/m = 3.6, 4.9 \times 10^7$, respectively, $L/D = 5.6, 9$ • $W/D = 2$ • At $M_\infty = 0.8$ & 1.4, $Re/m = 3.15 \times 10^7$, cavity dimensions doubled 	<ul style="list-style-type: none"> • Used leading edge fence and 0.03 in diameter cylindrical rod at various locations in BL for suppression 	<ul style="list-style-type: none"> • Shear-layer profiles suggest that rod works by “lifting” the shear layer and also by altering the mean shear layer • Cross-correlations of the sensors in the cavity suggest that the amplitude of the upstream traveling wave along the floor of the cavity was reduced slightly
Stanek et al. [41]	<ul style="list-style-type: none"> • Similar conditions as in Stanek et al. [19] 	<ul style="list-style-type: none"> • Investigated powered and unpowered resonance tubes, microjets vs. various other devices • Attempted to reduce mass flow requirements of mass flow devices 	<ul style="list-style-type: none"> • Proposed that hifex forcing alters the mean flow and its inviscid stability characteristics such that the growth of large-scale disturbances is prevented • Provides evidence that substantial amount of suppression in powered resonance tubes may be due to steady blowing effects (optimal $B_c \sim 0.6\%$)

Stanek et al. [42]	<ul style="list-style-type: none"> Similar conditions as in Stanek et al. [19] 	<ul style="list-style-type: none"> Investigated cylindrical rod in crossflow Investigated endcaps and fences 	<ul style="list-style-type: none"> Recommended optimal location is rod center at BL edge, optimal diameter is $2\delta/3$ Concluded that acoustic suppression is due to high-frequency rod shedding
Ukeiley et al. [56]	<ul style="list-style-type: none"> Similar conditions as in Ukeiley et al. [25] 	<ul style="list-style-type: none"> Investigated powered whistles (8) to superimpose hifex perturbations on ~horizontal steady blowing at the leading edge with heated air, nitrogen (28 kHz), and helium (78 kHz) 	<ul style="list-style-type: none"> Used B_c up to 0.4% but best results (factor of ~2–4 reduction in aft wall OASPL) were with lowest steady helium injection rate ($B_c \sim 0.09\%$) Suppression mechanism unclear; limited PIV images, and cross-correlation data suggest that injection alters impingement region and disrupts acoustic feedback loop
Zhuang et al. [1,50]	<ul style="list-style-type: none"> $M_\infty = 2$, $L/D = 5.1$, $L/W = 5.8$, $Re_L = 2.8 \times 10^6$ 	<ul style="list-style-type: none"> Investigated 400 μm diameter microjet array (12) with vertical injection 	<ul style="list-style-type: none"> Found $B_c = 0.1\text{--}0.5\%$ was sufficient for 5–11 dB reduction in OASPL and 13–28 dB peak reduction Saturation noted as B_c increased High reversed flow velocities (40–50% of the free stream) were observed in the middle and near the bottom half of the cavity
Sahoo et al. [53]	<ul style="list-style-type: none"> Similar conditions as in Zhuang et al. [50] 	<ul style="list-style-type: none"> Microjet actuators 	<ul style="list-style-type: none"> Developed physics-based model explanation of the effects of microjet blowing on supersonic cavity control
Schmit et al. [55]	<ul style="list-style-type: none"> $M_\infty = 0.85, 1.19$ $L/D = 5$ $W/D = 1$ 	<ul style="list-style-type: none"> Powered resonance tube Rod wrapped with wire Rotary pulse-blowing Sawtooth spoiler 	<ul style="list-style-type: none"> Direct comparisons of low- and high-frequency forcing did not show one method to be superior to the other Passive methods were ineffective at supersonic speeds
Williams et al. [66]	<ul style="list-style-type: none"> $M_\infty = 1.86$ $Re/m = 4.9 \times 10^7$ $L/D = 5$ $L/W = 1.5$ $\delta = 8 \text{ mm}$ 	<ul style="list-style-type: none"> Pulsed-blowing type of actuator with compressed air from siren valves Bandwidth of the device ~1.5 kHz 2-D slot orifice with height 3.2 mm $B_c = 0.13\%$ 	<ul style="list-style-type: none"> The overall supersonic cavity system performs as a linear system. Input disturbances are amplified when the external forcing frequency is close to that of a Rossiter mode, and attenuated when the external forcing frequency is between those of Rossiter modes.
Ukeiley et al. [49]	<ul style="list-style-type: none"> 3-D cavity with diverging side walls $M_\infty = 1.5$ $L/D = 5.5$ 	<ul style="list-style-type: none"> Eight 400 μm diameter jets evenly spaced along the leading edge of the cavity Different number of slots with different lengths and fixed width 0.254 mm $B_c = 0.1\text{--}0.55\%$ 	<ul style="list-style-type: none"> For microjet case, $B_c = 0.1\text{--}0.55\%$ was sufficient for 1–6 dB reduction in OASPL and 5–8 dB in peak reduction. For 2-D slot case, up to 7 dB reduction in OASPL

In 1999, three new approaches were reported. Fabris and Williams [37] used unsteady bleed (zero-net mass-flux) forcing to produce a broadband actuator capable of producing a complex input disturbance comprised of multiple frequency components. They demonstrated that the shear layer was most receptive to horizontal or tangential forcing via shear-layer velocity measurements, in contrast to the results of Shaw [36].

Lamp and Chokani [38] used a rotary-valve actuator to provide steady and/or oscillatory blowing upstream of the cavity leading edge at a particular pulsing frequency. Their actuator configuration emphasized three-dimensional effects and showed that oscillatory blowing can reduce tone amplitudes provided the forcing frequency is not a harmonic of the cavity resonance.

Raman et al. [39] and Raman and Raghu [40] used novel miniature fluidic oscillators to suppress cavity oscillations. These devices were capable of producing up to 3 kHz oscillations with mass flow rates of less than 0.12% of the main jet flow and produced significant tonal reductions. However, the mass flow rate and frequency of oscillations are coupled (albeit in a predictable fashion). Whether the steady mass additions or the unsteady oscillations were responsible for the sound suppression could not be determined. This is a key unresolved issue and, as emphasized in Ref. [13], independent control of the mean and oscillatory components is required.

Stanek et al. [19,41,42] reported on a series of larger-scale experiments conducted in the United Kingdom over the past few years. In the first experiment reported in 2000 [19], they investigated powered resonance tubes, protruding piezoceramic driven wedges, a cylindrical rod, and passive resonance tubes vs. a conventional spoiler. An interesting result was that the powered resonance tubes (see [23] and Section 3 below) demonstrated significant tonal and broadband reduction when $B_c \sim 1.6\%$. The result was termed a successful demonstration of high-frequency forcing (defined as a frequency that is very large compared to that of the cavity tones).

A follow-on study [41] reported in 2002 investigated powered and unpowered resonance tubes (in which the resonator tubes were blocked to inhibit high-frequency excitation), and microjets vs. various other devices. While the powered resonance tubes were redesigned to reduce their mass flow requirements, optimal suppression still required $B_c \sim 0.6\%$. The unpowered resonance tubes consistently provided the best suppression, indicating that the primary suppression mechanism of these devices is not just due to high-frequency forcing but is also influenced by the steady blowing component. The results also introduced microjet blowing, and showed that vertical blowing is required for these devices to be successful in this application.

Stanek et al. [41] offered a new explanation for the high-frequency forcing effect. The intrinsic idea was that high-frequency forcing alters the instability characteristics such that the growth of large-scale disturbances is inhibited or prevented. They hypothesized that the mechanism was a *decelerated* energy cascade in contrast to the findings of Wiltse and Glezer [43].

In 2003, Stanek et al. [42] reported various aspects of the cylindrical rod in crossflow. They studied the vertical position of the rod H/δ in the boundary layer, its relative size d/δ , installation issues, and end conditions. They recommended an optimal location as centered at the edge of the boundary layer and an optimal size of $d/\delta = 2/3$. They argued that their results conclusively demonstrate that the suppression is due to high-frequency forcing via vortex shedding from the cylinder. Additional arguments are provided in Ref. [44], which discusses the local stabilization of the shear layer via high-frequency forcing. While the cylinder clearly affects the mean flow and its stability characteristics, there are other important factors that cannot be ignored, including experimental evidence presented by Ukeiley

et al. [25] and the numerical simulations of Arunajatesan et al. [45], which indicate that the cylinder can also *lift* the shear layer and cause the impingement region to be altered. If the shear-layer impingement location is indeed altered, then the source strength is presumably affected.

It is clear that these studies provide insufficient information to sort out these different physical mechanisms. To do so requires confirmation in the form of detailed experiments, analysis, and validated simulations to determine the mean velocity profile and subsequent shear-layer instability characteristics for various high-frequency devices.

One other mechanism worth mentioning is the possibility of rod or wire resonance. A cylinder in crossflow can vary in complexity from a resonating string in tension [46] to a pinned or clamped rod in tension or compression (that can sustain bending) depending on its diameter, length, material, and boundary condition [47]. Sample calculations reveal fundamental resonant frequencies which can vary from several hundred hertz to several kilohertz, depending on the mounting configuration. If the wire/rod resonates due to the broadband excitation of the turbulent boundary layer and/or fluctuating pressure field, fluid/structure interaction effects, which have been ignored to date, may be significant.

There are a few other studies involving steady and/or pulsed blowing that have provided physical insight or have shown promising results. Bueno et al. [48] used an array of six fast-response (~ 3 ms) miniature jets mounted upstream of the leading edge to study the effects of normal injection on a Mach 2 cavity flow. They used instantaneous and ensemble-averaged pressure-time histories and cross-correlations to study the effects of single short and long cyclical pulses (50% duty cycle), the latter with relatively low forcing frequencies (50 or 80 Hz) compared to that of the tones. They compared their pulsed results to steady blowing with $B_c = 0.28\%$, 0.24% , 0.18% , and 0.16% at $L/D = 5, 6, 8,$ and 9 , respectively, and concluded that continuous mass injection is more effective for suppression than low-frequency pulsed blowing.

Ukeiley et al. [49] used an array of eight powered whistles mounted in the forward cavity wall as flow-control actuators. These devices essentially produce a high-frequency tonal oscillation superimposed on a steady jet. The jet is directed in the downstream direction but has a slight vertical velocity component. The authors studied the novel use of different injection gases (heated air, nitrogen, and helium) with and without the high-frequency “whistle” component. The best sound suppression results were obtained using steady helium blowing (no high-frequency component) with very low $B_c = 0.09\%$. The suppression mechanism requires further study, but sample Particle Image Velocimetry (PIV) images and cross-correlations of pressure-time histories suggest that the injection alters the impingement region and disrupts the acoustic feedback loop. Their results also highlight the need to rigorously study high-frequency forcing effects isolated from the mass flow injection from the actuator.

Zhuang et al. [50] investigated the use of a vertically directed microjet array mounted upstream of the cavity leading edge. The microjets had a 400 micron diameter and produced sonic jets that interact with the upstream boundary layer. The authors show how, at Mach 2, the microjets alter the cavity shear-layer thickness and the receptivity process, introduce streamwise vorticity, and alter the shear-layer trajectory and the resulting impingement region. Significant tonal and broadband suppression levels were achieved with B_c as low as 0.15% , which is significantly lower than the mass injection required in other studies using steady blowing. Higher levels of B_c produced no significant improvement.

Collectively, the blowing results described above indicate that manually optimized steady blowing configurations with $B_c \leq 0.2\%$ can be effective suppression devices. At subsonic speeds the primary mechanisms appear to be an alteration of the shear-layer stability characteristics, the introduction of streamwise vorticity, and modification of the shear-layer impingement location. While these are also important at supersonic speeds, shock wave/boundary layer interactions at the upstream cavity edge and the ensuing shear-layer trajectory alteration appear to be additional factors that should be considered.

It is interesting that when all of the available blowing data is expressed using the blowing coefficient definition of Vakili and Gauthier [31], one finds that the evolution of steady blowing techniques has reduced the effective (not necessarily optimal) B_c from $O(10\%)$ by two orders of magnitude down to $O(0.1\%)$. Note that the definition of B_c accounts for the cavity area but does not directly incorporate the scaling effects of the boundary layer. This has important implications for full-scale applications and is addressed further in Section 3. In comparison, low-frequency forcing does not appear to be very attractive when the actuator bandwidth is insufficient in comparison to the frequencies of the cavity tones. This is discussed further in Sections 3 and 5.

High-frequency excitation, whether it is passive or active, appears promising for both tonal and broadband suppression. However, the responsible mechanisms require further study. There is ample evidence that high-frequency forcing alters the mean flow. As a result, the shear-layer stability characteristics are altered and, in some cases, the trajectory of the shear layer is modified. When the impingement location is altered, the strength of the acoustic source is reduced and the broadband noise level decreases. As will be discussed in Section 5, to date closed-loop control produces comparatively little change in the mean-flow properties and, as such, has only been shown to be effective for tonal control.

2.3. Effect of control on the flow field and store trajectory

As discussed in the introduction, in addition to the increase in unsteady loads on the various aircraft structures, the highly oscillatory flow field generated by cavity flows can also adversely affect the safe departure and accurate delivery of stores from internal weapons bays. Such internal weapon bays are becoming more common in modern aircraft in large part due to the decreased aerodynamic drag and the lower radar signatures when compared to the external storage of weapons in earlier aircraft. Also, as mentioned earlier, this issue is becoming more pressing due to the increased reliance on smaller, and thereby lighter, munitions that are more susceptible to the large-scale oscillations in cavity flows that can lead to undesirable store separation [19]. Although more acute at supersonic speeds [51], this issue is still of

concern for stores released from internal bays at high subsonic speeds [52].

It is reasonable to assume that reducing cavity resonance, as measured by the reduction in p_{rms} inside and near the cavity, would have a favorable effect on the release of stores from internal bays. This is because the flow–acoustic coupling that governs cavity resonance (see Section 1) implies that a reduction in the dynamic pressures should be concomitant with a decline in the flow-field unsteadiness in terms of the fluctuating velocities. Recent studies, by Zhuang et al. [1] of supersonic flow over rectangular, three-dimensional cavities (i.e., not spanning the width of the test section), and that of Ukeiley et al. [49] using non-rectangular cavity configurations, provide direct evidence of this correlation between the unsteady pressures and the global velocity field. The use of normally oriented, microjet arrays by Zhuang et al., which led to reductions of up to 10 dB in the overall unsteady pressure level (OASPL) and more than 20 dB in the tonal amplitudes, also dramatically reduced the fluctuating velocities inside the cavity.

Fig. 5 from Zhuang et al. [50] illustrates the dramatic effect of flow control on the unsteadiness of the global flow field. These measurements were obtained using planar two-component PIV for Mach 2 flow over an $L/D \sim 5$ cavity. Here, Fig. 5a shows the contour plot of v_{rms} , the unsteady vertical component of the velocity for the baseline uncontrolled case, while Fig. 5b corresponds to the case with microjet control. As seen in Fig. 5a, very high rms intensities, as much as 10% of the free stream velocity, are observed inside baseline cavity. However, the microjets reduce the fluctuation intensities in the velocity field. Flow control not only reduces the magnitude of fluctuating intensities, by a factor of two or more in some regions, but also reduces the spatial extent of the region where the flow is highly unsteady. As shown by Ukeiley et al. [25] and Zhuang et al. [1,50] among others, various open-loop control approaches modify the mean-flow properties. These include (1) significant changes in the flow field inside the cavity, especially the reversed flow region; (2) modification of the cavity shear-layer thickness, especially in the initial, highly receptive region; and (3) a change in the shear-layer growth rate and/or its position relative to the trailing edge.

Although it is a rather intuitive inference that a reduction in the velocity fluctuations inside the cavity (due to flow control) should enhance store separation characteristics, the details of the fundamental mechanisms behind this relationship—including the influence of changes in the mean-flow field—are still not completely clear. Some factors to be considered include:

1. a reduction in the flow unsteadiness provides the store with more repeatable and stable initial conditions compared to the uncontrolled case and reduces disturbances that affect the store trajectory after it is released;

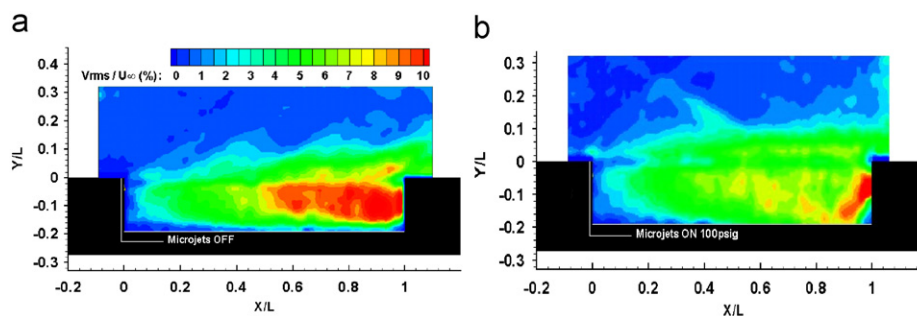


Fig. 5. Velocity-field measurements showing the effect of control on the flow unsteadiness, from Zhuang et al. [50]. Contours of v_{rms} with (a) no control and (b) microjet control.

- a change in the mean profile of the shear layer can alter the forces and moments encountered by the store, especially as it traverses a finite-thickness shear layer.

Clearly, more fundamental and comprehensive studies are needed that correlate the flow-field properties—and its response to control—to store dynamics. These can then be used to gain a better understanding of the flow physics governing this complex phenomenon and to develop more robust models that predict store trajectory. Such an attempt was recently made by Sahoo et al. [53] who built upon the extensive dynamic models of store release trajectory developed by Shalev et al. [52]. In particular, Sahoo et al. [53] developed a low-order model to predict store dynamics for stores released from internal bays exposed to supersonic flow. Using slender-body dynamics, their model only considers pitch and plunge motion of the store. It also contains several other simplifications—in large part to make the analysis more tractable—such as assuming the cavity to be quiescent, which is not always the case as documented in numerous studies cited in this article.

A noteworthy aspect of their model is that, where available, experimental data are incorporated to better capture store dynamics. For example, the effect of shear-layer profile/thickness is evaluated using velocity-field measurements from Zhuang et al. [50]. Furthermore, their dynamic model also attempts to capture the effect of the primary parameters that influence control efficacy on store trajectory in experimental studies. For example, the impact of varying C_{μ} , the steady momentum coefficient, has been incorporated. The model predictions are finally compared to store trajectory data obtained from supersonic free-drop tests conducted at the Boeing Polysonic Wind Tunnel [51]. Although the predictions do not agree with the details of the measured store trajectory; the model captures some of the overall trends. More importantly, it does accurately predict the success or failure of control in achieving a safe store departure from the weapons bay. Considering the many simplifications inherent in Sahoo's model, such agreement implies that there is hope for developing more sophisticated models that more accurately predict store dynamics in a quantitative sense.

Even though the details of the relationship between cavity flow oscillations and store trajectory are not well understood, the favorable impact of effective cavity/noise control on trajectory has been demonstrated in the free-drop tests at Boeing Polysonic Wind Tunnel [51]. An example of this can be seen in the sequence of high-speed, instantaneous Schlieren images shown in Fig. 6 [51]. The cavity is located on the top, and the store is ejected out of the cavity in the downward direction. The images on the left correspond to the baseline or no-control case, while those on the right correspond to a case where cavity oscillations (quantified via pressure spectra inside the cavity) have been significantly reduced using active flow control. Repeated free-drop tests demonstrate that without flow control, the store develops an undesirable pitch-up moment and returns to the cavity (bay) for most cases. However, the activation of flow control leads to an overall pitch-down moment on the store, leading to a safe departure.

A better understanding of the store dynamics can be achieved only through additional, careful experimental studies that provide high-fidelity, time-resolved measurements, such as synchronized velocity-field and pressure data or velocity combined with store trajectory measurements. Such data would enable the incorporation of more relevant physics into store dynamics and would also serve as a benchmark for validation of CFD simulations.

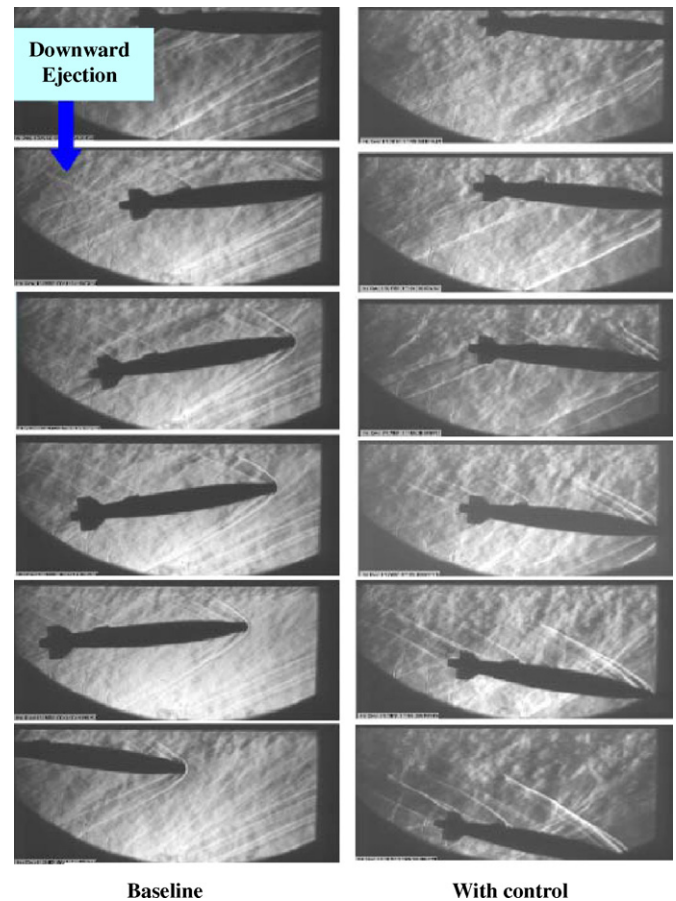


Fig. 6. High-speed instantaneous shadowgraphs, showing the favorable effect of control on store trajectory (from Bower et al. [51]).

3. Sensors and actuators

In general, actuators for cavity tone suppression are devices that act to disrupt some element of the acoustic resonance mechanism. Actuators may be a component of a closed-loop control system or act independently in an open-loop or passive mode. The cavity tones are suppressed when successful, but in some cases the broadband noise level is reduced as well [24]. Examples of actuators, their strengths and weaknesses, and the issues associated with their application will be discussed in this section.

3.1. Passive actuators

Passive actuators attenuate tones by changing the characteristics of the shear flow over the cavity. Passive actuators require few, if any, moving parts and tend to be inexpensive and simple devices. However, they often do not work well at off-design conditions [54,55]. When effective, passive actuators disrupt the resonance through one of at least three mechanisms:

- (1) the trajectory of the mean shear layer is changed such that the reattachment point is shifted downstream of the cavity edge [25,45,48],
- (2) the stability characteristics are modified by changes in the shear-layer velocity profiles and/or gas properties [12,56], so that the resonant modes are not amplified, and
- (3) the spanwise coherence of the shear layer and corresponding Rossiter mode is disrupted [45].

Examples of passive actuators include leading-edge ramps [32], spoilers [57], fences [25], steady gas injection [31], or contouring of the trailing edge of the cavity [20]. Spoilers and fences are commonly installed on production aircraft to reduce the resonant tones in weapons bays and deploy when the bay doors open. The fences act to increase the shear-layer thickness, which shifts the most unstable shear-layer frequencies to lower values. Spoilers and ramps deflect the mean separation streamline higher into the flow so that reattachment occurs downstream of the cavity trailing edge. This weakens the feedback acoustic wave and the resulting strength of the Rossiter modes.

Similarly, as shown in Fig. 7, rods placed in the upstream boundary layer produce a mean wake (momentum deficit), which modifies the mean shear-layer development [25,42,45]. Ukeiley et al. [25] studied both rods and variable-height fences and found the effect of the device on the *mean gradient* of the shear layer to be important in determining the level of attenuation.

3.2. Active open-loop actuators

Actuators that require energy to operate and, in turn, add energy to the flow are defined as active control devices. The term “open loop” emphasizes that a feedback signal is not used to control the actuator output. Examples include oscillating electro-mechanical [32,57,58] and piezoelectric flaps [19,35,59–62], steady blowing [32,48,63,64], and pulsed blowing [27,36,65,66], voice-coil drivers [67,68], powered resonance tubes [19,23,69,70], fluidic oscillating jets [39], and plasma actuators [71]. All of these open-loop actuators have demonstrated control of cavity resonance at subsonic flow conditions, but only the powered resonance tube and the steady and pulsed jets and microjets have been successful at supersonic free stream conditions.

It is important to recognize that a mean component of forcing is associated with most unsteady actuators. Even in the case of actuators that have no net mass addition, there will be a net momentum flux associated with the second-order streaming effect [72]. Streaming is the steady, secondary flow component resulting from the quadratic nonlinear interaction of the unsteady flow components. Whether this effect is significant or not depends on the amplitude of the oscillations. Actuators with a nonzero mass addition, such as pulsed jets, siren valves, powered resonance tubes, fluidics, and whistles will have first-order mean-flow components with disturbance magnitudes that are comparable to or exceed the amplitude of the unsteady component.

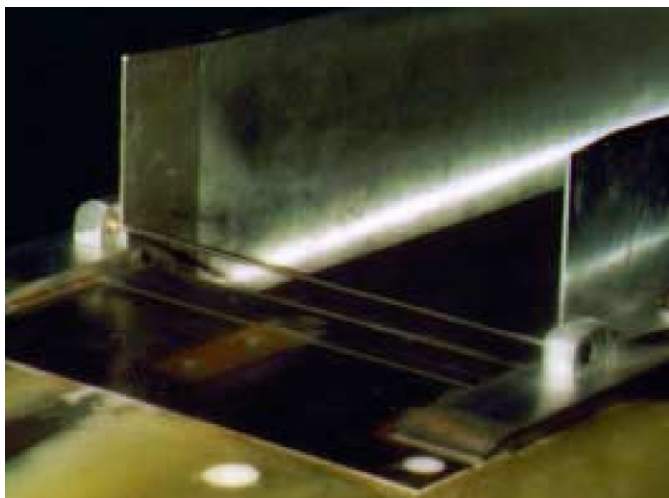


Fig. 7. Photograph of “CALSPAN95” cylindrical rod installed at the cavity leading edge (from Stanek et al. [42]). The vertical bay doors are deployed.

It is often a challenge to the actuator designer to maintain, for example, velocity fluctuation amplitudes at the same order-of-magnitude as the mean flow as the frequency increases. Because these devices have a strong mean component, it is often difficult to separate which component (i.e., mean or oscillatory) of actuation is responsible for the flow control.

As suggested by Stanek et al. [19] actuators can be further categorized into low-frequency excitation and high-frequency excitation (“hifex”). Hifex corresponds to forcing at an order-of-magnitude larger than the frequencies of the resonant tones, while low-frequency excitation corresponds to frequencies that are an order-of-magnitude or more less than the resonant tones. Sarno and Franke [32] proposed the concept of forcing the shear layer at a frequency different from that of the Rossiter mode as a way to suppress resonance. Because their actuators were limited to frequencies an order-of-magnitude lower than that of the first Rossiter mode, the results did not provide convincing evidence that the low-frequency forcing approach could be effective. By using a piezoelectric flap, Cattafesta et al. [35] were the first to clearly demonstrate that forcing the shear layer to oscillate at a frequency different from that of the Rossiter modes could result in noise attenuation in a low-speed cavity flow. Provided the excitation frequency was not in a narrow band near a Rossiter mode, in which case lock-on resonance occurred, the piezoelectric flaps were able to attenuate the mode by exciting shear-layer instabilities incommensurate with the Rossiter resonance mechanism. The non-Rossiter shear-layer modes grow at the expense of the natural Rossiter modes, indicating a nonlinear process. The effectiveness of this approach at higher Mach numbers is questionable due to the increasingly larger mean-flow energy available [66]. Wider bandwidth voice-coil type actuators have been used by Little et al. [73] to explore the effects of open-loop sinusoidal forcing at Mach 0.3.

Actuation at frequencies an order-of-magnitude larger than the Rossiter modes can also lead to suppression of the cavity tones via hifex. In particular, the technique pioneered by McGrath and Shaw [24] and revisited by others has suppressed tones at supersonic flow conditions. One hifex hypothesis [19] argues that energy addition to the shear layer at length scales much smaller than the coherent shear-layer vortices will directly increase dissipation and accelerates the turbulent energy cascade. Based on the results of numerical simulations of oscillatory (i.e., ac only) and pulsed (i.e., dc and ac) jets, Stanek [44] argues that hifex results in a local stabilization of the cavity shear layer to low-frequency perturbations and, in turn, cavity oscillations. Stabilization is observed to occur only when the pulsing frequency is above a critical threshold, in which case the input pulse rapidly decays.

Note that hifex can be achieved via passive control with rods mounted in the upstream boundary layer, as shown in Fig. 7, due to passive high-frequency vortex shedding or via active control (with, for example, powered whistles and powered resonant tubes shown in Fig. 8 and described in Refs. [56,74]). A typical hifex experiment will produce disturbances in the range of 5 kHz or higher in order to suppress tones in the 500 Hz range or lower. However, the physics of the hifex effect are difficult to sort out, because all hifex actuators realized to date also have a substantial effect on the mean flow that can influence the shear-layer development, its impingement location, and the acoustic source. The mean-flow-modification effect using rods in crossflow has been demonstrated by Ukeiley et al. [25] and Arunajatesan et al. [45]. As mentioned above, Stanek [44] and, even earlier, Rizzetta and Visbal [75] have shown, via large-eddy simulations in a Mach 1.19 cavity, that pure high-frequency oscillatory forcing can suppress cavity oscillations, but no reported experiments have been able to corroborate this hypothesis. Hence, this remains an open question and warrants additional research.

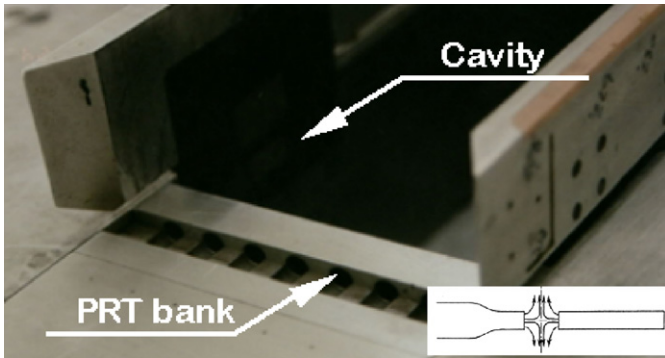


Fig. 8. Photograph of an array of powered resonance tubes (PRT) installed at the leading edge of the cavity in a similar installation as in Fig. 7. The inset shows a schematic of a single actuator. Adapted from Stanek et al. [74].

Regardless of the type used, active open-loop actuators are attractive because of their relative simplicity and ability to be activated when needed. However, Shaw and Northcraft [27] demonstrated the sensitivity of the control effect to forcing frequency and changing flow conditions. Open-loop actuators, like passive actuators, must be optimized for each flow condition. Furthermore, Cattafesta et al. [35] demonstrated with piezoelectric flap actuators at the cavity leading edge that an order-of-magnitude higher power is required to drive open-loop actuators compared to closed-loop systems for equivalent reductions. Similar power penalties with other open-loop actuators are expected.

3.3. Active closed-loop actuators

Actuators for closed-loop control form part of a system that includes at least one flow state sensor and a feedback control algorithm. This approach is the most expensive in terms of hardware and complexity, but it offers the greatest adaptability to changing flow conditions and potentially the lowest power consumption. A summary of some actuators used in closed-loop cavity control experiments is provided in Table 2. Again, the investigations are listed in chronological order for historical purposes.

Closed-loop actuators for active control of cavity oscillations also fall into two types. A “Type A” actuator is a device with sufficient bandwidth that is capable of producing, at any instant in time, a control input consisting of several frequencies, each with its own amplitude and phase. This type of actuator has a time response commensurate with the time scales of the cavity flow dynamics so that it can be used in a dynamic feedback compensation scheme. A voice-coil actuator is an example of a Type A actuator (see Table 2). A “Type B” actuator is also a broadband device, but it produces a control signal of prescribed amplitude and *primarily* one fundamental frequency (with perhaps harmonics and a mean-flow component) at any instant in time. The actuator frequency can change only on a time scale that is large compared to the time scales of the cavity flow dynamics. Shaw and Northcraft [27] successfully used this approach with a rotary-valve, pulsed-blowing actuator. At any instant in time, the rotor spins at a particular rotation rate (rpm), and the supply pressure has a certain value. These can both be changed via, for example, a control voltage to a dc motor and servo valve, but the slow time response due to its finite inertia precludes a rapid change in the actuator output or the ability to phase lock with the acoustic field.

The majority of closed-loop, flow-control experiments summarized in Table 2 use Type A actuators [35,68,76–90]. When

feedback is used to control the flow, then the dynamics of the flow system are changed. Unlike open-loop control, the transfer function of the actuator plays a major role in how the overall system will behave. For example, the bandwidth of the actuator plays a crucial role in determining the maximum achievable performance from the closed-loop system, as a consequence of the *area rule* discussed in Section 4.4. The bandwidth should ideally be large enough to suppress more than one Rossiter mode. Otherwise an actuator with small bandwidth cannot attenuate a resonant peak without amplifying undesirable neighboring modes [81]. For this reason, it is important to know the actuator transfer function when designing a closed-loop control algorithm. More details will be given in Section 4, and techniques to estimate the transfer function for piezoelectric flaps and synthetic jets are described, for example, in Refs. [59,91], respectively.

Initially the closed-loop actuator must have enough power to produce a disturbance that exceeds the receptivity-induced perturbation at the upstream end of the cavity. After the system responds to the actuation, the actuator power requirements decrease with the decreasing tone amplitudes. Cattafesta et al. [35] demonstrated the initial high-amplitude piezoelectric flap actuator output (see Table 2) reduced by an order-of-magnitude after control was established.

To date there has not been a demonstration of closed-loop control (Type A) at supersonic speeds. Shaw and Northcraft [27] demonstrated that both open-loop and Type B closed-loop control were capable of controlling the tones and reducing the broadband noise levels with pulsed-fluidic injection at supersonic speeds. The challenge associated with closed-loop control is to achieve similar noise reductions with an order-of-magnitude lesser input power by using Type A actuators. Actuators with large amplitudes, high bandwidth, and fast time response are therefore required, which raises the issue of actuator scaling. Shaw [92] studied the mean mass flow rate requirements for a pulsed injection system directed perpendicular to the free stream and determined that the steady momentum coefficient $c_{\mu} = \dot{m}U_{\text{jet}}/(q_{\infty}W\delta)$ collapsed two sets of data at Mach 0.95, with frequencies ranging from 100 to 600 Hz and widely varying δ and q_{∞} . Note that the area in the denominator is the width of the cavity multiplied by the boundary layer thickness at the leading edge of the cavity. This scaling parameter was used successfully for weapons bay cavity flow control in the flight test of an F-111 [93]. More recently, in experiments ranging from small (model scale <3%) laboratory scale tests to large industrial scale models, where model scale is >10% of full scale, Zhuang et al. [50], Ukeiley et al. [49], and Bower et al. [51] have determined that the steady momentum coefficient is the most relevant scaling parameter for fluidic actuator design. It appears to capture the fundamental parameters governing the efficacy of actuators in reducing the cavity dynamic loads, as well as the flow unsteadiness.

For the purposes of Type A flow-control actuation with piezoelectric flaps or with zero-net mass-flux actuators, the momentum coefficient will need to include the fluctuating component of velocity, presumably as an oscillatory momentum coefficient $c_{\mu} = \rho_{\text{jet}}u_{\text{rms}}^2A_{\text{jet}}/(q_{\infty}W\delta)$. But the problem of designing a wide bandwidth actuator that works effectively at high subsonic Mach numbers is exacerbated by the quadratic dependence of the dynamic pressure $q_{\infty} = 0.5\gamma p_{\infty}M_{\infty}^2$ on Mach number. In conventional pressure-driven tunnels, where increasing subsonic Mach numbers are achieved by increasing the stagnation pressure, p_{∞} is approximately constant and is on the order of the atmospheric pressure. Because the tones are stronger than the broadband noise, the actuator authority must also increase with Mach number in a similar manner. For example, using c_{μ} -based scaling, the dynamic pressure increases by a factor of nine as the Mach number increases by a factor of three for a fixed static pressure.

Table 2
Summary of selected actuators used for closed-loop control

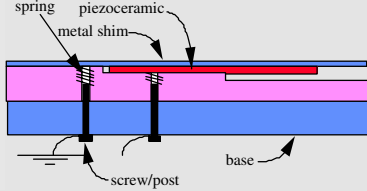
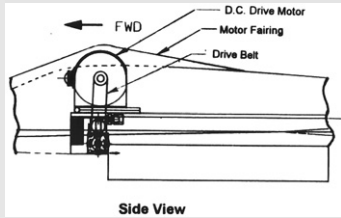
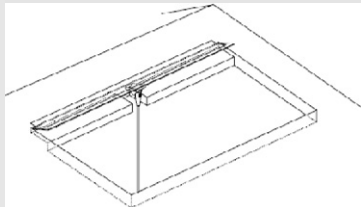
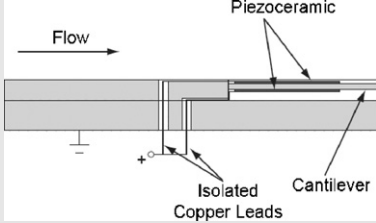
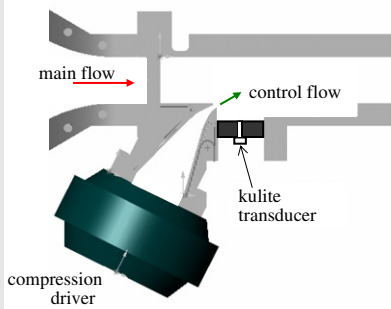
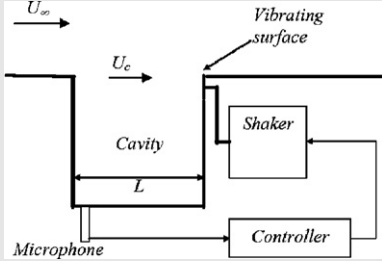
Study	Conditions	Method of actuation	Control approach	Power (W)	Comments
Cattafesta et al. [35]	<ul style="list-style-type: none"> $U_{\infty} = 40\text{m/s}$, $L/D = 0.5$, $L/W = 0.5$, $Re_{\theta} = 4750$, $L/\theta = 81$ $U_{\infty} = 45\text{m/s}$, $L/D = 2.0$, $L/W = 2.0$, $Re_{\theta} = 5210$, $L/\theta = 328$ $W = 12\text{ in}$, $D = 6, 12\text{ in}$ 	<ul style="list-style-type: none"> Unimorph piezoelectric flaps at leading edge $f_{\text{typ}} \approx 300\text{ Hz}$ $23\ \mu\text{m/V}$ @ 300 Hz 	<ul style="list-style-type: none"> Type A 		<ul style="list-style-type: none"> Comparison of open-loop voltage and closed-loop voltage requirements
Shaw and Northcraft [27]	<ul style="list-style-type: none"> $M_{\infty} = 0.6\text{--}1.05$ $L/D = 6.46$, $L/W = 3.67$ 	<ul style="list-style-type: none"> Pulsed fluidic at leading edge, 90° w.r.t. flow Frequency $< 650\text{ Hz}$ 	<ul style="list-style-type: none"> Type B Mass flow and frequency adjusted based on rms levels within 3 frequency bands 		
Cattafesta et al. [29]	<ul style="list-style-type: none"> $M_{\infty} = 0.4\text{--}1.35$ $L/D = 5$ 	<ul style="list-style-type: none"> Piezoelectric flaps at cavity leading edge $f_{\text{res}} \approx 475\text{ Hz}$ $2.5\ \mu\text{m/V}$ @ 500 Hz 1.875 mm max disp. 	<ul style="list-style-type: none"> Type A Adaptive disturbance rejection controller 		<ul style="list-style-type: none"> Feedback signal is pressure near leading edge of cavity
Mongeau et al. [57]	<ul style="list-style-type: none"> $U_{\infty} = 14\text{--}29\text{ m/s}$ Partially closed cavity, 1/5 scale car model 	<ul style="list-style-type: none"> Oscillating spoiler hinged at leading edge of cavity opening Voicecoil driver Max. 1 mm displacement @ 120 Hz 	<ul style="list-style-type: none"> Type A Loop shaping of open-loop transfer functions measured on system components 	< 100	<ul style="list-style-type: none"> Digital control using Simulink® Real-Time Workshop
Williams et al. [28]	<ul style="list-style-type: none"> $M_{\infty} = 0.25\text{--}0.55$ $L/D = 5$ 	<ul style="list-style-type: none"> Zero-net-mass flow oscillations through leading edge slot, 0° w.r.t. flow Two 500 W, 8 in speakers $f_{\text{typ}} \approx 340\text{ Hz}$ 	<ul style="list-style-type: none"> Type A Model-based control with 2nd-order bandpass filters 	0.33–53 depending on control	<ul style="list-style-type: none"> Feedback signal from cavity floor at $x/L = 0.8, 0.875$
Ziada [77]	<ul style="list-style-type: none"> $M_{\infty} = 0.3$ $L/D = 2.5, 4$ $L = 127, 203\text{ mm}$ $D = 50.8\text{ mm}$, $W = 76\text{ mm}$ 	<ul style="list-style-type: none"> Synthetic jet through leading edge slot, 45° w.r.t. flow Two 50 W, 100 mm diameter speakers 	<ul style="list-style-type: none"> Type A Time delay and gain applied to feedback signal 		

Table 2 (continued)

Study	Conditions	Method of actuation	Control approach	Power (W)	Comments
Kegerise et al. [84–86]	<ul style="list-style-type: none"> • $M_\infty = 0.275$ • $L/D = 5$ 	<ul style="list-style-type: none"> • Bimorph piezoelectric flap at cavity leading edge • $f_n \sim 1200$ Hz • DC gain $\sim 0.25 \mu\text{m/V}$ 	<ul style="list-style-type: none"> • Type A • Generalized predictive control 	1	
Cabell et al. [83]	<ul style="list-style-type: none"> • $M_\infty = 0.275, 0.35, 0.45$ • $L/D = 5$ • $L/W = 3$ 	<ul style="list-style-type: none"> • Piezoelectric-driven type of synthetic jet actuator with $44.5 \text{ mm} \times 0.5 \text{ mm}$ 2-D slot orifice. • Peak velocity at slot exit is $\geq 15 \text{ m/s}$ over 60–1500 Hz. 	<ul style="list-style-type: none"> • Type A • Linear Quadratic control design using the state-space models computed from experimental data. 		
Debiasi and Samimy [76,87]	<ul style="list-style-type: none"> • $L = 50.8 \text{ mm}, W = 50.8 \text{ mm}$ • $L/D = 4$ • $\delta = 2.5 \text{ mm}$ • $Re_\delta = 2 \times 10^4, M_\infty = 0.25\text{--}0.5$ 	<ul style="list-style-type: none"> • Zero-net mass-flux forcing of the shear layer at the leading edge through a slot ($50.8 \text{ mm} \times 1 \text{ mm}$) at 30° w.r.t. flow • A compression driver with bandwidth 1–20 kHz 	<ul style="list-style-type: none"> • Type A • Logic-based controller with forcing frequency between 2 and 5 kHz and fixed amplitude 		
Micheau et al. [107]	<ul style="list-style-type: none"> • $L = 800 \text{ mm}, W = 150 \text{ mm}$ • $L/D = 5.3$ • $Re_L = 3 \times 10^5, M_\infty = 0.11$ 	<ul style="list-style-type: none"> • A vibrating surface (3 cm by 3 cm) with a shaker located at the trailing edge 	<ul style="list-style-type: none"> • Type A • Envelope controller 		
Rowley et al. [129]	<ul style="list-style-type: none"> • $L = 152.4 \text{ mm}, W = 76.2 \text{ mm}$ • $L/D = 2$ • $M_\infty = 0.6, L/\theta = 52.8$ 	<ul style="list-style-type: none"> • Zero-net mass-flux forcing at the leading edge • 200 W compression driver • Exponential horn design 	<ul style="list-style-type: none"> • Type A • Heuristic feedback control law 		

This implies that the actuator rms velocity fluctuation level will need to increase by a factor of three to be effective. Perhaps a more realistic scenario for actuator development would employ a wind tunnel that allows independent control of Mach number and q_∞ to simulate the actual flight environment. Until such actuators and experiments are available, numerical simulations can and should be used to study virtual actuator scaling requirements.

Finally, we note a reported discrepancy for the optimal injection angle. As summarized in Table 1, Shaw [36] has found that vertical injection is superior for pulsed blowing at low frequencies, while Williams et al. [28] and Kegerise et al. [84] find horizontal injection is superior for Type A zero-net mass-flux actuators. Stanek et al. [41] have found that steady microjets have been effective only in vertical injection configurations. The reason for this observed discrepancy is unclear and again warrants further careful studies.

3.4. Sensors and flow measurements

Since the aim of most cavity control experiments is to reduce the pressure fluctuations, unsteady pressure sensors are commonly used in laboratory control applications. Lou et al. [94] used microphones, with their lower noise floor and reduced full-scale range, to measure (and control) the flow-induced pressure oscillations due to an impinging jet. But the unsteady pressure levels inside a cavity often exceed the linear full-scale range of microphones, forcing the use of unsteady pressure transducers. By far the most common sensors used to examine cavity flows are miniature, high-frequency-response piezoresistive pressure transducers, such as those made by Kulite, Endevco, and PCB Piezotronics.

These transducers are usually flush mounted or recessed beneath a pinhole—to achieve better spatial resolution at frequencies well below the Helmholtz frequency of the recessed cavity/pinhole combination. They are usually mounted on one of the cavity surfaces, generally the floor and/or the leading and trailing surfaces. Alternatively, they are placed in the tunnel walls [89] near the cavity to measure the near acoustic field ($<$ one acoustic wavelength from the trailing edge). The small size, linearity (output voltage linearly proportional to input pressure), their flat-frequency response over a large frequency range, and their high dynamic range (ratio of maximum-to-minimum detectable pressure) make them an excellent tool for characterizing the cavity dynamics. Such transducers have been used to examine subsonic [95], supersonic [50], and hypersonic [96] cavity flows. They have been used in small-scale, laboratory facilities and in larger commercial testing facilities [41,94].

In order to better understand the global flow behavior, one must look beyond the surface pressure or acoustic field. The dynamics of cavity flows have been examined using a number of other diagnostic tools. For example, relatively low Mach number cavity flows have also been examined using constant-temperature hot-wire anemometry. Shear-layer profiles (mean and fluctuating) and, in some cases, instability growth rates have been obtained. Examples can be found in Mendoza and Ahuja [33], Hsu and Ahuja [34], Cattafesta et al. [35], Garg and Cattafesta [97], Kegerise [98], and Williams and coworkers [28,37,66,67,80,95].

Hot-wire anemometry becomes increasingly problematic in high-speed flows due to wire breakage and compressibility effects [99]. Consequently, other techniques have been used. For example, Little et al. [73] and Samimy et al. [89] have used hot-film probes. Vakili et al. [100] used a multi-hole probe to obtain upstream boundary layer profiles as a function of mass injection. Kegerise [98], Kegerise et al. [101], and Garg and Cattafesta [97] characterized the spatio-temporal behavior of high-speed, sub-

sonic, cavity flows using a combination of fluctuating pressure measurements and phase-conditioned measurements of the density field inside the cavity using a quantitative, non-intrusive Schlieren instrument. The quantitative Schlieren technique (and hot wires) was used to study nonlinear mode interactions and mode switching [28,102]. Zhuang et al. [50] also used a combination of Schlieren and shadowgraph methods along with unsteady surface pressure measurements to study supersonic cavity flows. Such data provide invaluable information regarding the spatio-temporal nature of the events that dominate the cavity dynamics and can provide insight concerning nonlinear interactions and model switching.

Similarly, Forestier et al. [103] have studied transonic (Mach 0.8) flow over deep cavities ($L/D \sim 0.4$) using high-speed Schlieren photography to visually examine the periodic component of the cavity shear-layer oscillations. In addition, they obtained phase-locked laser Doppler velocimetry measurements to examine the evolution of periodic and spatially coherent structures (or vortices) extracted from the velocity-field data. Murray and Elliott [104] have used Schlieren photography and planar laser imaging of supersonic cavity flows (1.8–3.5) to study the characteristics of cavity shear-layer structures. Little et al. [73] and Samimy et al. [89] have used phase-locked planar laser imaging to visualize the organized structure of various baseline and open-loop controlled cavity flows at Mach 0.3.

Some investigators have used PIV with varying degrees of success to study high-speed cavity flows [50,56,89,105]. Most of the difficulties are associated with proper seeding of the cavity flow. Zhuang et al. [50] have obtained velocity and vorticity fields in a supersonic flow and have examined the effects of microjet control (see Fig. 5).

With regard to safe separation of stores from military aircraft, one wishes to predict the trajectory, based on a simple measurement, such as the fluctuating pressures inside the cavity. To accomplish this, correlations between measurements made inside the cavity and on the store are required. Such a database can be created through captive trajectory tests, where forces and moments on the store are measured simultaneously with the unsteady pressures inside the cavity. Another approach is the use of sensors, such as accelerometers, gyros, and inclinometers, which measure the pertinent store trajectory parameters. Stores embedded with such sensors combined with telemetry data systems can then be used to obtain and correlate the signals. Further discussion on the effect of control on store trajectory and recent efforts on modeling this behavior were discussed in Section 2.3.

4. Closed-loop control methodologies

The active control suppression studies described in Section 2 used open-loop techniques. Here, we summarize several studies (see Table 3) that used closed-loop control, which incorporates some type of feedback from a sensor placed in the flow. As categorized in the diagram in Fig. 3, one way to use this feedback is to “tune” an inherently open-loop approach, for instance by slowly modulating the frequency and amplitude of open-loop forcing (labeled *quasi-static*) to achieve the best suppression in a quasi-static or time-averaged sense. A different way is to use feedback at the time scale of the dynamics (labeled *dynamic*). This latter approach can have even more beneficial effects, such as even lower power required for control.

Open-loop control cannot alter the dynamics of a system (e.g., stabilize an instability) except by exciting nonlinearities (e.g., by modifying the mean flow). This implies a large power requirement, either as power explicitly supplied to an actuator, or

Table 3
Summary of selected closed-loop cavity suppression studies

Study	Conditions	Method	Comments
Gharib [106]	<ul style="list-style-type: none"> • $U_\infty = 22$ cm/s, $Re_D = 24,000$, laminar BL $H = 2.5$, $Re_\theta = 95$ • $L/\theta = 66, 77, 82$ 	<ul style="list-style-type: none"> • Strip heater used to excite TS waves via Joulean heating 	<ul style="list-style-type: none"> • Feedback control using manual gain and phase adjustment reduced rms fluctuations by factor of 2
Cattafesta et al. [35]	<ul style="list-style-type: none"> • $L/D = 0.5$, $L/W = 0.5$, $U_\infty = 40$ m/s, $L/\theta = 81$ • $L/D = 2.0$, $L/W = 2.0$, $U_\infty = 45$ m/s, $L/\theta = 328$ 	<ul style="list-style-type: none"> • Used piezoelectric flaps mounted at the leading edge of the cavity to suppress low-speed cavity oscillations • Used LQG and pole-placement feedback control designs 	<ul style="list-style-type: none"> • CL control suppressed oscillations with order-of-magnitude lesser input actuator power • Shear-layer meas. w/ & w/o control show no effect on mean flow
Mongeau et al. [78,79]	<ul style="list-style-type: none"> • $U_\infty = 15$–29 m/s flow over a Helmholtz resonator 	<ul style="list-style-type: none"> • Used active spoiler driven via a moving coil loudspeaker (up to ~ 1 mm or less than 1°) • Used robust loop shaping algorithm 	<ul style="list-style-type: none"> • Significant attenuation achieved with small actuation effort • Robust performance for transient operating conditions
Kestens and Nicoud [109]	<ul style="list-style-type: none"> • Laminar BL with $Re_\delta = 1000$ and $L/D = 2$ for $M_\infty = 0.2$ 	<ul style="list-style-type: none"> • 2-D NS simulations • Used off-line system identification for system transfer function model • Used filtered-X algorithm 	<ul style="list-style-type: none"> • Demonstrated suppression only in vicinity of microphone • No effect on flow (active noise control, not active flow control)
Cattafesta et al. [29]	<ul style="list-style-type: none"> • $L/D = L/W = 5$ • $M_\infty = 0.4, 0.6, 0.85$ • Calculated $\delta = 10.5$ mm @ $M_\infty = 0.6$, $Re/m = 11 \times 10^6$ 	<ul style="list-style-type: none"> • Used piezoelectric flaps flush at the leading edge of the cavity • Used adaptive disturbance rejection algorithm & system identification 	<ul style="list-style-type: none"> • Demonstrated successful single-tone suppression at $M_\infty = 0.74$, $L/D = 4$, $L/W = 3$ small-scale test but negligible suppression in larger-scale wind tunnel tests
Shaw and Northcraft [27]	<ul style="list-style-type: none"> • $L/D = 6.46$, $L/W = 3.67$ • $M_\infty = 0.6, 0.85, 0.95, 1.05$ 	<ul style="list-style-type: none"> • Tested pulsed fluidic injection at the cavity leading edge using closed-loop control via rotary valve • Quasi-steady tuning of open-loop fixed-frequency forcing based on bandpass-filtered rms pressure signal 	<ul style="list-style-type: none"> • Controller optimizes injection mass flow rate and frequency • Suppression of tones demonstrated but new tones appear at excitation frequency
Williams et al. [28]	<ul style="list-style-type: none"> • $L/D = 2.4$, or 5, $L/W = 1.33$ • $M_\infty = 0.2$–0.55, $\delta = 3.18$–2.41 cm, $\theta = 0.30$–0.26 cm 	<ul style="list-style-type: none"> • Used zero-net mass-flux unsteady bleed actuator to suppress or enhance individual resonant cavity modes • Used analog output feedback 	<ul style="list-style-type: none"> • Experiments showed 0° forcing was better than 45° or 90° (vertical) • Multiple-mode suppression at $M_\infty = 0.48$ • Studied nonlinear mode interactions
Williams et al. [67]	<ul style="list-style-type: none"> • Similar conditions as above • BL data: at $M_\infty = 0.2$–0.55, $\delta = 3.18$–2.41 cm, $\theta = 0.30$–0.26 cm 	<ul style="list-style-type: none"> • Used zero-net mass-flux unsteady bleed actuator used to suppress or enhance individual resonant modes • Used analog output feedback control circuit 	<ul style="list-style-type: none"> • Found single-mode resonance can occur if cavity mode coincides with Rossiter mode • at Mach 0.35, input power from 6.3 W (suppressed oscillations) to max. of 53 W • Could suppress or enhance tones
Williams and Morrow [95]	<ul style="list-style-type: none"> • Similar to above • $L/D = 5$, $L/W = 1.33$ • $M_\infty = 0.25$–0.55 	<ul style="list-style-type: none"> • Used a commercial adaptive digital controller from Arbor Scientific as a follow-on to earlier work • Used filtered-X LMS algorithm 	<ul style="list-style-type: none"> • Comparable results for single-mode analog controller suppression but unable to suppress multiple modes simultaneously • Suggested need for adaptive plant model
Williams et al. [80] & Rowley et al. [81,82]	<ul style="list-style-type: none"> • Similar to above • $L/D = 5$, $L/W = 1.33$ • $M_\infty = 0.34$, 	<ul style="list-style-type: none"> • Companion papers to study model-based control of cavity oscillations • Experiments used feedback control to suppress the mode and then perform frequency-response exp. • Feedback controller is 2nd-order Butterworth filter with different bandwidths, gain, and time delay 	<ul style="list-style-type: none"> • Cavity can exhibit limit-cycle behavior or act like a stable noise amplifier • Discussed peak splitting via Nyquist analysis, fundamental performance limitations of feedback control using area rule

Cabell et al. [83]	<ul style="list-style-type: none"> • $M_\infty = 0.275, 0.4, 0.6$ • $L/D = 5, L/W = 3$ s at $M_\infty = 0.275$, $\delta \sim 5\text{--}6$ mm 	<ul style="list-style-type: none"> • Application of discrete-time, Linear Quadratic control design methods to the cavity tone problem • Used ERA to obtain state-space model via system identification • Piezosynthetic jet actuator at leading edge directed parallel to free stream 	<ul style="list-style-type: none"> • System model required $\sim 150\text{--}200$ states • Control order reduced to ~ 60 states using balance realization truncation • Frequency-shaping technique used to restrict controller frequency range • Peaking and peak splitting observed—features explained via linear models
Kegerise et al. [84]	<ul style="list-style-type: none"> • $M_\infty = 0.275, 0.4, 0.6$ • $L/D = 5, L/W = 3$ s at $M_\infty = 0.275$, $\delta \sim 5\text{--}6$ mm 	<ul style="list-style-type: none"> • Used piezoceramic bimorph flap actuator to suppress multiple cavity tones using output feedback control • Assessed IIR- and FIR-based system identification plant models 	<ul style="list-style-type: none"> • Demonstrated multiple modes • Found required actuator tip motion for suppression varied by 6–17 wall units • FIR model not suitable for plant model, IIR model required
Debiasi et al. [87]	<ul style="list-style-type: none"> • $L = 50.8$ mm, $W = 50.8$ mm • $L/D = 4$ • $\delta = 2.5$ mm • $Re_\delta = 2 \times 10^4$, $M_\infty = 0.25\text{--}0.5$ 	<ul style="list-style-type: none"> • Zero-net-mass-flux forcing of the shear layer at the leading edge through a slot (50.8 mm \times 1 mm) of 30° w.r.t. flow • A compression driver with bandwidth 1–20 kHz • Logic-based controller with forcing frequency between 2 and 5 kHz and fixed amplitude 	<ul style="list-style-type: none"> • The peak pressure fluctuations were suppressed up to 23 dB • Effectiveness of the controller was reduced at high Mach number (above 0.4) flow presumably due to the lack of actuation authority
Micheau et al. [107]	<ul style="list-style-type: none"> • $L = 800$ mm, $W = 150$ mm • $L/D = 5.3$ • $Re_L = 3 \times 10^5$, $M_\infty = 0.11$ 	<ul style="list-style-type: none"> • A vibrating surface (3 cm by 3 cm) with a shaker located at the trailing edge • Envelope controller 	<ul style="list-style-type: none"> • Single peak reduction can achieve up to 25 dB
Kegerise et al. [85,86]	<ul style="list-style-type: none"> • $L = 152.4$ mm • $W = 50.89$ mm • $L/D = 5$ • $\delta = 6$ mm 	<ul style="list-style-type: none"> • Piezoelectric bimorph cantilever beam at leading edge • Bandwidth ~ 1 kHz • $f_n \sim 1200$ Hz • DC gain ~ 0.25 $\mu\text{m/V}$ • Off-line system ID • Adaptive generalized predictive control 	<ul style="list-style-type: none"> • Demonstrated multiple Rossiter mode suppression at fixed Mach numbers ranging 0.275–0.38 • Concluded that the disturbances entering the cavity flow were collocated with the control input at the cavity leading edge
Yan et al. [88]	<p>Similar conditions as in Debiasi et al. [87]</p>	<ul style="list-style-type: none"> • Linear controllers such as H_∞, Smith predictor, PID, and PID-based parallel proportional with time delay controllers were implemented 	<ul style="list-style-type: none"> • Controller design was based on the linear model introduced in Williams et al. (2002) and Rowley et al. (2002) • Rapid switching occurred between the Rossiter modes by the forcing of linear controllers • Adding a zero to the linear controller can cancel the newly excited Rossiter mode
Samimy et al. [89]	<p>Similar conditions as in Debiasi et al. [87]</p>	<ul style="list-style-type: none"> • Linear Quadratic optimal controller 	<ul style="list-style-type: none"> • Controller design was based on reduced-order models derived using POD method along with the Galerkin projection method • 1000 Simultaneous PIV-pressure measurements were used for POD calculations
Efe et al. [132]	<p>Similar conditions as in Debiasi et al. [87]</p>	<ul style="list-style-type: none"> • Direct and indirect synthesis of the neural architectures to identify and control the system 	<ul style="list-style-type: none"> • The performance of the neurocontroller was not satisfactory • $1.6V_{\text{rms}}$ produced a 20 dB reduction of the resonant peak at the expense of the excitation of a large sideband peak
Rowley et al. [129]	<ul style="list-style-type: none"> • $L = 152.4$ mm, $W = 76.2$ mm • $L/D = 2$ • $M_\infty = 0.6$ • $L/\theta = 52.8$ 	<ul style="list-style-type: none"> • Zero-net-mass-flow forcing at the leading edge • One 200 W compression driver with 900 W amplifier • Exponential horn design • Heuristic feedback law 	<ul style="list-style-type: none"> • Feedback control was introduced into 2-D direct numerical simulations

as a drag penalty. By contrast, closed-loop control can linearly stabilize a system (i.e., with “infinitesimal” actuation), and furthermore it can reduce the amplification of external disturbances, such as boundary layer turbulence or external acoustic waves. In addition, adaptive techniques may be used to tune the controller’s behavior in real time.

4.1. Quasi-static vs. dynamic controllers

The first closed-loop approaches were modifications of open-loop strategies. We categorize these strategies as *quasi-static*, because in these approaches, the time scales by which feedback acts are much slower than the time scales of the flow. In perhaps the first known closed-loop cavity control experiments, Gharib [106] used periodically forced strip heaters to excite Tollmien–Schlichting waves in the boundary layer upstream of a cavity. By feeding back a velocity measurement from a downstream location in the cavity, and phase locking the sinusoidal forcing to this measurement, they obtained a 40% reduction in velocity fluctuations.

Shaw and Northcraft [27] also used feedback to modulate a sinusoidal forcing function. They measured the unsteady pressure level in a bandpass-filtered signal and then used an iterative search algorithm to adjust the frequency and amplitude of a pulsed-jet actuator and achieved a significant suppression of the tones, along with some suppression of broadband noise. Micheau et al. [107] used a feedback envelope controller to drive a vibrating surface located at the trailing edge of the cavity. In their experiment, the single peak resonance was reduced by up to 25 dB. Debiasi and Samimy [87] also used an adaptive learning approach, in which open-loop forcing is applied at a particular frequency, and this frequency is automatically adjusted by a learning algorithm to obtain the best suppression.

The class of closed-loop control that we call *dynamic* controllers uses feedback at the time scales of the unsteady motion of the fluid. This type of control is most amenable to techniques from classical and modern control theory and has some distinct advantages over modulated open-loop techniques, as discussed at the beginning of this section. Since the majority of recent closed-loop control studies have used dynamic controllers, the remainder of this section focuses on these.

Nearly all of the dynamic closed-loop cavity control studies to date have used linear control techniques. While this might seem restrictive, it is actually reasonable to expect that linear controllers would perform well. The reasons for this are twofold. First, recent experiments have indicated that in some regimes, purely linear mechanisms can describe even finite-amplitude oscillations of the cavity [80–82]. Second, even in regimes in which nonlinearities play a role in the naturally oscillating cavity, one hopes that in the controlled cavity, the oscillations will be small, and thus linear models will remain valid.

4.2. Models

Most linear control approaches rely on an accurate mathematical model of the system to be controlled. In this setting, the cavity flow is viewed as an input–output system, where the input is, for instance, the voltage signal supplied to the actuator, and the output is a sensor measurement. There may be multiple sensors, or even multiple actuators, in which case the input and/or output are vectors. Many different modeling techniques have been used in recent years, either based on flow physics or empirically identified directly from an experiment, and we describe some of these techniques below.

4.2.1. System identification

Several studies have determined a model for the cavity flow empirically using input/output data. The general approach is to force the cavity system, comprising the actuator(s), cavity, sensor(s), and any signal conditioners (e.g., amplifiers, filters), over a broad range of frequencies, measure the response from the sensor, and then either determine an empirical transfer function from spectra, or use an adaptive filter approach [108] to tune coefficients in a filter such that the mean squared error signal between the filter and the data is minimized (see Fig. 9). In the first case, the model is a frequency-response function, which may be expressed via Bode or Nyquist plots. In the second case, a time-domain discrete filter is used. In either situation, a linear model takes the form of a rational transfer function, whose coefficients are ultimately determined either off-line via a least-squares approach or on-line in a recursive fashion, for instance using a gradient descent algorithm such as least mean squares (LMS) or recursive least squares (RLS) [108]. Once a model is obtained, many standard tools for control system design may be used. Several approaches are described below.

As an example of the frequency-response method, Mongeau et al. [78] and Kook et al. [79] estimated open-loop transfer functions for low-speed flow past a Helmholtz resonator at several different flow velocities. A similar approach was used by Rowley and Williams [68], who obtained an empirical transfer function for a compressible cavity flow. An important difference in this work was that a manually tuned controller was used to first stabilize the oscillations prior to performing the frequency-response experiment. The frequency-response experiment was performed on the stabilized system, and then the effect of the known controller was removed. The reason for this approach is that a frequency-response experiment makes sense only for stable linear systems. If the system is unstable, with the amplitude of oscillation limited by nonlinearities, then it is not clear how to interpret the results of the frequency-response experiment. The distinction between a lightly damped, but stable cavity system, vs. a self-sustained cavity oscillation is discussed further in Ref. [13].

Several system identification techniques have been used to determine models in the form of rational transfer functions or state-space representations. Most of these involved frequency-response experiments on the uncontrolled cavity, and as mentioned above, if the linearized system is indeed unstable, and the

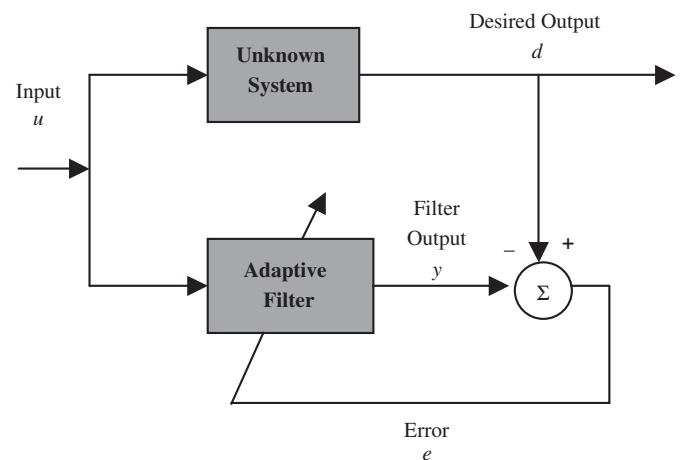


Fig. 9. Schematic of system identification approach using adaptive filters to obtain a low-order dynamical system model. A broadband input signal is supplied to the unknown cavity plant and the filter with unknown coefficients. The error signal from the filter is fed back to adjust the filter coefficients to minimize the mean square error signal.

oscillations are self-sustained, then the meaning of such experiments is not clear.

Kestens and Nicoud [109] used a filtered-X LMS algorithm to determine a model for a two-dimensional Navier–Stokes simulation of a forced cavity flow. The model was determined with no flow, so effects such as shear-layer convection and amplification would not be captured by such a system identification.

Cattafesta et al. [35] used an off-line least-squares method to identify the parameters in a discrete-time difference equation, and then used an eigensystem realization algorithm to convert this to state-space form [110]. Cabell et al. [83] used a similar approach and obtained state-space models of very high order (150–200 states). In these experiments, low coherence was observed between input and measured signals in the system identification experiment, so long time records (> 10 s) were required. Controllers designed from these models yielded reasonably good suppression, and the models predicted general trends observed in the experiments.

Cattafesta et al. [29] and Kegerise et al. [84] subsequently used an on-line adaptive system identification algorithm together with an adaptive feedback controller. In this case, an independent random signal is added to the computed control signal so that the system model can be updated while the adaptive controller is active. Such closed-loop system identification avoids the problem mentioned above of identifying an unstable system. Adaptive identification algorithms, including extensions to nonlinear system models, are discussed further in Pillarisetti and Cattafesta [111]. Nonlinear models provide greater model accuracy at the expense of increased computational complexity. The resulting nonlinear model can either be linearized and used with standard linear control schemes, or they can be used with nonlinear control schemes.

4.2.2. POD/Galerkin models

The system identification procedures described above treat the cavity as a black box, and models are obtained by observing the response to forcing. An alternative approach is to obtain models based solely on the physics of the flow system. The advantage of this approach is that it can provide insight into the mechanisms of cavity oscillations that might not be apparent otherwise. In addition, one may obtain scaling laws that determine how the models vary as a parameter such as Mach number or cavity length is varied.

The governing equations for most fluids are the Navier–Stokes equations, so in a sense a very accurate model of cavity flows is already known. However, standard tools for control analysis and design do not apply to nonlinear partial differential equations. So in order to use these techniques, it is desirable to approximate the Navier–Stokes equations by a finite-dimensional system. An increasingly popular method for obtaining such low-dimensional models is Proper Orthogonal Decomposition (POD) and Galerkin projection. In this method, data from simulations or experiments are used to determine a finite-dimensional subspace that contains the “most important” features of the flow (based on energy). The Navier–Stokes equations are then projected onto this subspace to obtain a low-dimensional model. For a comprehensive review of this method, see Holmes et al. [112].

POD/Galerkin models for 2-D flow past a cavity were demonstrated by Rowley et al. [113,114], and POD modes were also determined by Ukeiley et al. [115]. Similar models were obtained from experimental data and used for control design by Samimy et al. [89] and Caraballo et al. [90]. The standard method for incompressible flows needs to be modified for compressible flows, in which case the thermodynamic variables become important. It has been found that vector-valued POD modes work better than

scalar-valued POD modes. However, to use vector-valued modes, one must choose an inner product that appropriately weights the thermodynamic variables (e.g., density) and kinematic variables (e.g., velocity). See Rowley et al. [116] for a thorough description of the method for compressible flows.

The result of the Galerkin projection is a set of nonlinear ordinary differential equations. A key issue is that the standard Galerkin model does not explicitly include the control input. This limitation can be addressed in various ways, and Samimy et al. [89] provide an example application of a spatial subdomain separation method in a subsonic cavity flow application. The experimental implementation of the resulting controller requires real-time updates of the state variables (coefficients of the POD modes) based on sensor measurements, and various methods for such state estimation are discussed in Section 4.3.1.

4.2.3. Rossiter-type models

In contrast to POD models, in which the full Navier–Stokes equations are simplified, another approach is to model different components of the Rossiter mechanism, and connect these together, building more complex models from simple models of the individual components. Cain et al. [117] used a nonlinear model for shear-layer amplification, coupled with models for acoustic scattering and receptivity, to predict amplitudes of cavity oscillations. Their procedure was iterative, and provided an estimate for steady-state amplitude, but was not time-accurate. Nonetheless, it represented a significant improvement over the basic Rossiter model [2] and the more advanced Tam and Block [118] model.

Rowley and Williams [68] and Rowley et al. [82] used purely linear models for the various components as shown in Fig. 10, including shear-layer amplification, and obtained time-accurate models in the form of transfer functions. The model suggested an alternative mechanism for cavity oscillations: while the conventional view is that the oscillations are self-sustained; an alternative view is that the cavity could act as a lightly damped oscillator that amplifies noise at resonant frequencies. In this case, the oscillations are not self-sustaining. The linear models obtained in their paper explained some peak-splitting effects observed in experiments, and implied some fundamental performance limits [13], as discussed in Section 4.4.

The models described above provide physical insight, but without empirical tuning, they are not sufficiently accurate to design a control system. Recently, Kerschen and Tumin [119], Alvarez et al. [120], and Alvarez and Kerschen [121] described a theoretical model of cavity resonance that shows promise for physics-based cavity control design. It combines a propagation model based on a finite-thickness shear layer with scattering models for the leading and trailing-edge regions of the cavity using an exact Wiener–Hopf technique. The model predicts the cavity resonance frequencies without any empirical constants and also provides the temporal growth rate of each mode. It has also been used to demonstrate the effect of tunnel modes [13].

4.3. Control algorithms

This section discusses dynamic-control algorithms, in which the feedback occurs at the time scales of the unsteady flow. The simplest control strategies do not require a model, and the parameters of the controller are tuned manually. Williams et al. [28] used such a strategy, in which a pressure signal was bandpass filtered about the frequency of a cavity tone, and a phase shifter was manually tuned until the oscillations were suppressed. Several bandpass filters were used in parallel to achieve suppression of multiple modes, and a similar approach was used by

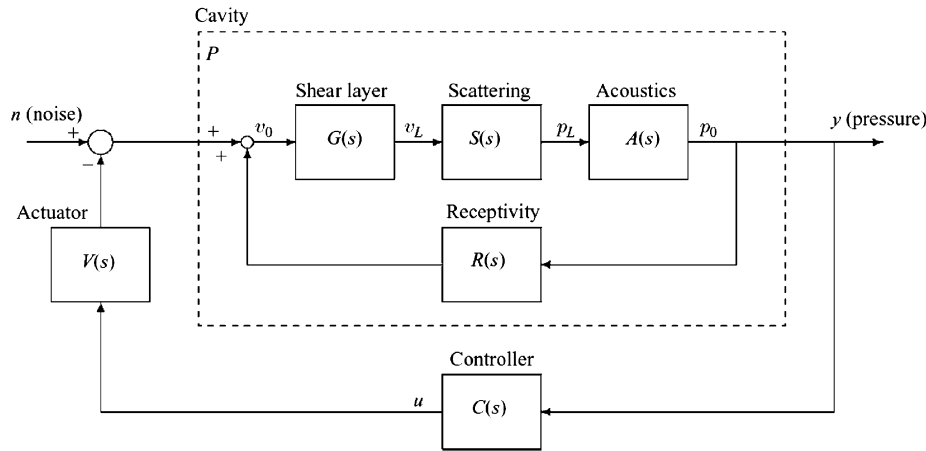


Fig. 10. Physics-based model of cavity oscillations that uses a linear model (i.e., transfer function) for each component of the system (from Rowley et al. [82]).

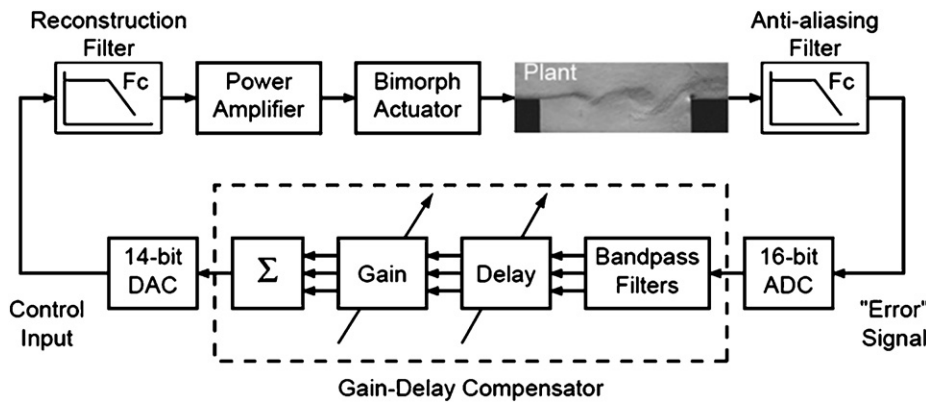


Fig. 11. Control architecture to bandpass filter each cavity tone of interest and feed back a scaled and delayed version of each for maximum suppression (from Kegerise et al. [84]).

Kegerise et al. [84] to suppress multiple modes, as illustrated in Fig. 11.

While manual tuning of controller parameters can work reasonably well, often new tones are produced by the controller. Furthermore, obtaining good suppression with manual tuning is usually difficult, especially when multiple modes are present and the actuator bandwidth is limited. More predictable design methodologies are available if one has a model of the system. For instance, Mongeau et al. [78] and Kook et al. [79] used a classical loop-shaping technique to design a control law for the flow past a Helmholtz resonator. Given a plant model $P(s)$, then with a controller given by $C(s)$, where $s = i\omega$, one may design the loop gain $L(s) = P(s)C(s)$ such that the closed-loop system has some desired properties, such as good disturbance rejection over a certain frequency range (characterized by the sensitivity function described in Section 4.4). One then determines $C(s)$ by inverting the plant: $C(s) = L(s)/P(s)$. If the plant model has zeros or poles in the right-half plane (RHP), then in order to avoid undesirable RHP pole-zero cancellation, one must place certain restrictions on $L(s)$, which can be cumbersome (see Doyle et al. [122] for more details).

Modern control tools provide systematic ways of designing controllers, given an adequate model [123]. Two types of optimal control design, discussed below, are the Linear Quadratic Regulator (LQR), used when the full state vector is available, and Linear Quadratic Gaussian (LQG), when only noisy sensor measurements are available. Cattafesta et al. [35] used LQG, as

well as pole placement (also discussed below), to suppress the oscillations with an order-of-magnitude lesser input power than open-loop techniques. Cabell et al. [83] also used an LQG regulator, with a frequency-dependent weighting on the control effort. The models used for these control designs were identified directly from experimental data. POD/Galerkin models have also been used for control design using LQR, in direct numerical simulations [129] and experiments [89,90]. However, controllers based on POD/Galerkin models often suffer from limitations in the model fidelity. In the simulations, for example, careful tuning of the LQR weights was necessary to achieve suppression of tones, and the performance of the model on full simulations did not match the behavior of the reduced-order model. In the experiments, the gains needed to be reduced by an adjustable multiplicative factor to avoid actuator saturation. These results highlight the need for developing methods to provide more accurate reduced-order models and also to adapt or update the model in an automated fashion as the system moves along a trajectory from its baseline to controlled state.

For both pole placement and LQG, one begins with a model or realization of the system in state-space form:

$$\begin{aligned} \dot{x}_{k+1} &= Ax_k + Bu_k, \\ y_k &= Cx_k + Du_k, \end{aligned} \quad (2)$$

where u_k is the input (actuator voltage) at time $t_k = k \Delta t$, and y_k is the corresponding output (sensor measurement). Here x_k is the

state vector, and A – D are matrices of appropriate dimension. If one chooses a feedback law

$$u_k = Kx_k, \quad (3)$$

where K is a matrix of gains, then the closed-loop system becomes

$$\begin{aligned} x_{k+1} &= (A + BK)x_k, \\ y_k &= (C + DK)x_k. \end{aligned} \quad (4)$$

A basic fact from control theory is that if the realization is controllable, the matrix K may be chosen to place the eigenvalues of $A+BK$ at any desired locations. Thus, even if the original system is unstable (i.e., the eigenvalues of A lie outside the unit circle), K can be chosen such that the closed-loop system is stable, and in fact such that the response decays arbitrarily quickly. This design approach is called *pole placement*; one specifies the desired locations of the closed-loop poles, and solves for the gains K that achieve them. The tradeoff in control design is to choose K to achieve a balance between fast response (good) and large values of the gains (bad). Large gains require large actuator power and amplify sensor noise.

An optimal way of achieving this balance between fast response and large gains is to use a Linear Quadratic Regulator (LQR) [124], which chooses K to minimize a cost function

$$J = \sum_{k=0}^{\infty} (x_k^T Q x_k + u_k^T R u_k), \quad (5)$$

where Q and R are symmetric, positive-definite matrices. The first term is related to the performance, while the second term provides a measure of the cost of the control input. These matrices are the parameters in the control design, and by choosing different matrices we choose how to balance good performance against the cost of control. One determines the value of the gain matrix K that minimizes this cost function by solving a quadratic matrix equation (an algebraic Riccati equation), and there are commercial software tools available to do this.

4.3.1. State estimation: observers and static estimators

In order to use the state feedback techniques described above, one needs to know the state x_k , which usually is not directly available. For instance, in a POD model, the state x_k consists of the amplitude of each POD mode, which usually cannot be measured directly. In order to obtain the state, one typically designs an observer to estimate the state, for instance by solving the equation

$$\hat{x}_{k+1} = A\hat{x}_k + Bu_k + L(C\hat{x}_k + Du_k - y_k), \quad (6)$$

where \hat{x}_k is the state estimate at time t_k and L is a matrix of observer gains. One may choose these observer gains such that the estimate is guaranteed to converge to the actual state (as long as the realization is observable). Again, there is a tradeoff between fast convergence and large amplification of sensor noise, and an optimal way of balancing these tradeoffs uses a procedure that precisely parallels LQR. Such an optimal observer is called a Kalman filter. When a Kalman filter is combined with state feedback using LQR, the resulting controller is called an LQG regulator. For more information about LQR and LQG regulators, see standard controls texts [124–126].

An alternative approach is to use a *static* estimator, such as Linear Stochastic Estimation (LSE), originally proposed by Adrian [127]. In this approach, the state estimate depends only on the sensor measurements at the present time, unlike the above *dynamic* approach, which has a memory of the time history of the sensor measurements. An extension of LSE to include quadratic terms for improved accuracy has been successfully employed by Murray and Ukeiley [128] and Samimy et al. [89] in cavity flows.

In LSE, the state estimate is represented by a static linear function of the sensors

$$\hat{x}_k = My_k, \quad (7)$$

where the matrix M is determined by correlating known states x with their corresponding sensor measurements y . This technique does not require a model but requires a larger number of sensors, and is more sensitive to noise than dynamic observers such as (6) [129]. Extensions to quadratic stochastic estimation provide a significant improvement over (7) but still require a large number of sensors [128,130]. For these reasons, we strongly endorse the use of dynamic observers such as (6) vs. static estimators such as (7), even if only a crude model of the dynamics is available. For cavity flows, an observer of the form (6) was used by Rowley and Juttijudata [131] to reproduce the first few POD modes in a direct numerical simulation, using a single noisy pressure sensor.

Adaptive disturbance rejection control techniques have also been used, in which parameters of the controller are updated in real-time in order to drive the sensor measurements to zero. Such controllers have been used by Kestens and Nicoud [109], Cattafesta et al. [29], and Keizerize et al. [86] with good success. One promising area for future research lies in the combination of adaptive physics-based system identification combined with adaptive control. The idea here is to replace the “black-box” model with a physics-based model but update the model (and the controller) with experimental data.

4.4. Fundamental limits on achievable performance

Though closed-loop controllers have provided reasonably good suppression, they often produce some adverse effects, such as an increase in noise at other frequencies. For instance, if the gain of a controller is increased too much, then a peak-splitting phenomenon may be observed as shown in Fig. 12 (Rowley et al. [81] and Cattafesta et al. [29]), in which the main resonant peak splits into two peaks on either side of the original peak. Because of fundamental limitations of feedback control, such adverse effects are unavoidable to some extent, though they may be minimized by the controller design as described below.

In Fig. 4 with unity gain feedback $H(s) = 1$, the transfer function from an external disturbance to the output is given by

$$\frac{P(s)}{1 + P(s)C(s)} = S(s)P(s), \quad (8)$$

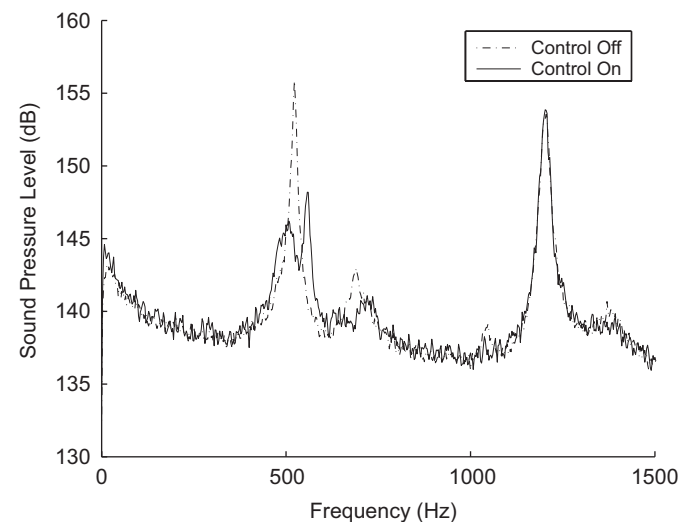


Fig. 12. The reduction of the first cavity at Mach 0.74 illustrates the peak-splitting phenomenon (from Cattafesta et al. [29]).

where $S = 1/(1+PC)$ is the *sensitivity* function. Since the transfer function from disturbances to output for the open-loop (i.e., no-control) system is simply $P(s)$, the sensitivity function is the ratio of the closed-loop to open-loop transfer functions and, hence, quantifies how feedback alters the effect of disturbances. One of the goals of feedback design for cavity flows is to reduce the amplification of disturbances, so we would like to make $|S(i\omega)| < 1$ for all frequencies $\omega \in \Re$. Unfortunately, this is not possible in a linear control system, due to Bode's integral formula, or *area rule*, which states that if the relative degree of the loop gain is at least 2 (i.e., the degree of the denominator of $P(s)C(s)$ is at least 2 greater than the degree of the numerator, which is virtually always true in practice), then

$$\int_0^{\infty} \log |S(i\omega)| d\omega = \pi(\log e) \sum_i \operatorname{Re}(p_i), \quad (9)$$

where p_i denotes the RHP poles of $P(s)C(s)$. For instance, if the plant is stable (i.e., the right-hand side of the equation is zero), then in a log-linear plot of $|S(i\omega)|$, the area of attenuation ($|S(i\omega)| < 1$) must be balanced by an equal area of amplification ($|S(i\omega)| > 1$), in which the closed-loop system amplifies disturbances even more than the open-loop one. If the plant is unstable, the area of amplification must be larger than the area of attenuation. Of course, all of this attenuation and amplification must occur within the bandwidth of the controller, since $|S(i\omega)| = 1$ when the control goes to zero. Hence, narrow bandwidth controllers or actuators will have severe limitations. If good performance is desired at one frequency, then a penalty of bad performance at other frequencies within the passband must be incurred. Wider bandwidth actuators will not have such severe limitations, since the area of amplification may be spread out over a large frequency range. This emphasizes yet again the need to develop high-bandwidth actuators.

5. Summary and outlook

This paper has provided a review of active control of flow-induced cavity oscillations, where emphasis has been placed on recent experimental investigations of open- and closed-loop suppression techniques. It is worth noting that, with a few exceptions, most of the experimental results available in the literature and discussed herein have been obtained from studies conducted in relatively small facilities. There have been some questions regarding the value of such studies at “impractically small” scales as to whether they capture the key flow physics encountered in the “real/full-scale” world. However, comparison of results obtained in small-scale experiments with those at larger scales has clearly shown that at least as far as cavity flows are concerned, these experiments do capture the relevant flow physics and can be accurately scaled to larger facilities and flight tests provided care is taken to avoid tunnel modes [13]. More importantly, small-scale studies can be successfully used to design and scale actuators for large-scale tests—see, for example, Zhuang et al. [50] and Ukeiley et al. [49]. Since the costs associated with smaller scale studies are significantly lower, and the results obtained are more detailed, it is imperative that experiments at these small, research laboratory scales strive to achieve a better understanding of the fundamental flow physics governing cavity flows and their response to various actuation methods. Once better understood, the more promising concepts can be intelligently scaled for further validation at increasingly larger scale.

Based on the results discussed in this article, we conclude with the following observations/recommendations. First, while the suppression of cavity oscillations is an important problem of

practical interest, the search for a solution to this problem combined with budgetary, time, and scientific constraints often limits flow-physics experiments. Where possible, flow-field measurements (both mean and fluctuating components) should be conducted for the baseline and controlled cases. In addition, the interaction of the actuator with the flow should be characterized. Beyond improving our understanding of cavity oscillations, these data will provide the basis for future comparison and scaling results. It will also permit the evaluation of critical issues, for example, isolating high-frequency excitation vs. mean-flow-modification effects.

Furthermore, several active open-loop and passive schemes have demonstrated the ability to reduce broadband levels, while closed-loop control methods explored to date have not modified the mean flow significantly. Evidence suggests that broadband suppression implies a modification of the mean flow.

While the closed-loop results have been promising, only passive and active open-loop methods have been successful at supersonic speeds. It is conceivable that a hybrid scheme consisting of some combination may be effective. For closed-loop control to have an even greater impact, several things should occur. First, adaptive physics-based dynamic models are required to enable design of suitable controllers. Second, better “Type A” (discussed in Section 3) actuators are required that have higher output, larger bandwidth, and faster time response, such that multi-mode tonal (and perhaps broadband) closed-loop control at supersonic speeds is possible. Third, it is our opinion that researchers in the field of flow control must accept, if not embrace, the role of multiple disciplines (e.g., fluid dynamics, control theory, and transducers). Only in this manner can active flow control achieve its full potential.

Acknowledgements

The research program at Florida A&M University and Florida State University (FAMU-FSU) is supported by DARPA (Technical monitor: Dr. Steven Walker) and Boeing (Technical monitor: Dr. William Bower). The research at UF, IIT and Princeton has been supported by AFOSR (Technical monitors John Schmisser and Sharon Heise). The authors are grateful to Mr. Ning Zhuang for his help in reviewing some of the literature for this paper and would also like to acknowledge their collaborators on cavity flow work, Profs. A. Annaswamy (MIT) and C. Shih (FAMU-FSU), Larry Ukeiley (UF), and Tim Colonius (Caltech).

References

- [1] Zhuang N, Alvi F, Shih C. Another look at supersonic cavity flows and their control. AIAA 2005-2803, May 2005.
- [2] Rossiter JE. Wind-tunnel experiments on the flow over rectangular cavities at subsonic and transonic speeds. Aeronautical Research Council Reports and Memoranda no 3438, October 1964.
- [3] Powell A. On edge tones and associated phenomena. *Acustica* 1953;3: 233–43.
- [4] Krishnamurty K. Acoustic radiation from two dimensional rectangular cutouts in aerodynamic surfaces. NACA Technical Note 3487, August 1955.
- [5] Roshko A. Some measurements of flow in a rectangular cutout. NACA Technical Note 3488, August 1955.
- [6] Rockwell D, Naudascher E. Review: self-sustaining oscillations of flow past Cavities. *Trans ASME J Fluids Eng* 1978;100:152–65.
- [7] Rockwell D, Naudascher E. Self-sustained oscillations of impinging shear layers. *Annu Rev Fluid Mech* 1979;11:67–94.
- [8] Rockwell D. Oscillations of impinging shear layers. *AIAA J* 1983;21(5): 645–64.
- [9] Blake WK, Powell A. The development of contemporary views of flow tone generation. In: *Recent advances in aeroacoustics*. New York: Springer; 1986. p. 247–345.
- [10] Komerath NM, Ahuja KK, Chambers FW. Prediction and measurement of flows over cavities—a survey. *AIAA* 87-0166, January 1987.

- [11] Chokani N. Flow induced oscillations in cavities—a critical survey. DGLR/AIAA 92-01-159, May 1992.
- [12] Colonius T. An overview of simulation, modeling, and active control of flow/acoustic resonance in open cavities. AIAA 2001-0076, January 2001.
- [13] Rowley CW, Williams DR. Dynamics and control of high-Reynolds number flow over cavities. *Annu Rev Fluid Mech* 2006;38:251–76.
- [14] Williams DR, Rowley CW. Recent progress in closed-loop control of cavity tones. AIAA 2006-0712, January 2006.
- [15] Bruggeman JC, Hirschberg A, van Dongen MEH, Wijnands APJ. Self-sustained aero-acoustic pulsations in gas transport systems: experimental study of the influence of closed side branches. *J Sound Vibr* 1991;150:371–93.
- [16] Kook H, Mongeau L, Brown DV, Zorea S. Analysis of the interior pressure oscillations induced by flow over vehicle openings. *Noise Control Eng J* 1997;45:223–34.
- [17] Srinivasan GR. Acoustics and unsteady flow of telescope cavity in an airplane. AIAA *J Aircr* 2000;37(2):274–81.
- [18] Jumper EJ, Fitzgerald EJ. Recent advances in aero-optics. *Prog Aerosp Sci* 2001;37:299–339.
- [19] Stanek M, Raman G, Kibens V, Ross J, Odedra J, Peto J. Control of cavity resonance through very high frequency forcing. AIAA 2000-1905, June 2000.
- [20] Heller HH, Bliss DB. The physical mechanisms of flow-induced pressure fluctuations in cavities and concepts for their suppression. AIAA 75-491, March 1975.
- [21] Shaw LL. Suppression of aerodynamically induced cavity oscillations. AFFDL-TR-79-3119, November 1979.
- [22] Chokani N, Kim I. Suppression of pressure oscillations in an open cavity by passive pneumatic control. AIAA 91-1729, June 1991.
- [23] Raman G, Cain AB. Innovative actuators for active flow and noise control. *Proc Instn Mech Eng G J Aerosp Eng* 2002;216:303–323.
- [24] McGrath SF, Shaw Jr LL. Active control of shallow cavity acoustic resonance. AIAA 96-1949, June 1996.
- [25] Ukeiley LS, Ponton MK, Seiner JM, Jansen B. Suppression of pressure loads in cavity flows. AIAA *J* 2004;42(1):70–9 See also AIAA 2002-0661.
- [26] DiStefano III JJ, Stubberud AR, Williams IJ. Feedback and control systems. In: Schaum's outlines. 2nd ed. New York: McGraw-Hill; 1990.
- [27] Shaw L, Northcraft S. Closed loop active control for cavity resonance. AIAA 99-1902, May 1999. See also Rothfuss DA, Northcraft SA. Active control of weapons bay acoustics. AFRL-VA-WP-TR-1998-3039, June 1998.
- [28] Williams D, Fabris D, Iwanski K, Morrow J. Closed loop control in cavities with unsteady bleed forcing. AIAA 2000-0470, January 2000.
- [29] Cattafesta III LN, Shukla D, Garg S, Ross JA. Development of an adaptive weapons-bay suppression system. AIAA 99-1901, May 1999.
- [30] Sarahia V, Massier PF. Control of cavity noise. *J Aircr* 1977;14(9):833–7.
- [31] Vakili AD, Gauthier C. Control of cavity flow by upstream mass-injection. *J Aircr* 1994;31(1):169–74.
- [32] Sarno RL, Franke ME. Suppression of flow-induced pressure oscillations in cavities. *J Aircr* 1994;31(1):90–6.
- [33] Mendoza JM, Ahuja KK. Cavity noise control through upstream mass injection from a Coanda surface. AIAA 96-1767, May 1996.
- [34] Hsu JS, Ahuja KK. Cavity noise control using Helmholtz resonators. AIAA 96-1675, May 1996.
- [35] Cattafesta III LN, Garg S, Choudhari M, Li F. Active control of flow-induced cavity resonance. AIAA 97-1804, June 1997.
- [36] Shaw L. Active control for cavity acoustics. AIAA 98-2347, June 1998.
- [37] Fabris D, Williams DR. Experimental measurements of cavity and shear layer response to unsteady bleed forcing. AIAA 99-0606, January 1999.
- [38] Lamp AM, Chokani N. Computation of cavity flows with suppression using jet blowing. *J Aircr* 1997;34(4):545–51.
- [39] Raman G, Raghu S, Bencic TJ. Cavity resonance suppression using miniature fluidic oscillators. AIAA 99-1900, May 1999.
- [40] Raman G, Raghu S. Cavity resonance suppression using miniature fluidic oscillators. AIAA *J* 2004;42(12):2608–12.
- [41] Stanek MJ, Raman G, Ross JA, Odedra J, Peto J, Alvi F, et al. High frequency acoustic suppression—the role of mass flow, the notion of superposition, and the role of inviscid instability—a new model (part II). AIAA 2002-2404, June 2002.
- [42] Stanek MJ, Raman G, Ross JA, Odedra J, Peto J, Alvi FS, et al. High frequency acoustic suppression—the mystery of the rod-in-crossflow revealed. AIAA 2003-0007, January 2003.
- [43] Wiltse JM, Glezer A. Direct excitation of small-scale motions in free shear flows. *Phys Fluids* 1998;10(8):2026–36.
- [44] Stanek MJ. A numerical study of the effect of frequency of pulsed flow control applied to a rectangular cavity in supersonic crossflow. PhD thesis, Department of Aerospace Engineering and Engineering Mechanics, University of Cincinnati, 2005.
- [45] Arunajatesan S, Shipman JD, Sinha N. Mechanisms in high frequency control of cavity flows. AIAA 2003-0005, January 2003.
- [46] Blackstock DT. Fundamentals of physical acoustics. New York: Wiley; 2000. p. 218.
- [47] Le KC. Vibrations of shells and rods. New York: Springer; 1999. p. 155–61.
- [48] Bueno PC, Ünalmsis ÖH, Clemens NT, Dolling DS. The effects of upstream mass injection on a Mach 2 cavity flow. AIAA 2002-0663, January 2002.
- [49] Ukeiley LS, Sheehan M, Coiffett F, Alvi FS, Srinivasan A, Jansen B. Control of pressure loads in complex cavity configurations. AIAA 2007-1238, January 2007.
- [50] Zhuang N, Alvi FS, Alkislal MB, Shih C. Supersonic cavity flows and their control. AIAA *J* 2006;44(9):2118–28 See also AIAA 2003-3101.
- [51] Bower WW, Kibens V, Cary AW, Alvi F, Raman G, Annaswamy A, et al. High-frequency excitation active flow control for high-speed weapon release (HIFEX). AIAA 2004-2513, June 2004.
- [52] Shalaev VI, Fedorov AV, Malmuth ND. Dynamics of slender bodies separating from rectangular cavities. AIAA *J* 2002;40(3):517–25.
- [53] Sahoo D, Annaswamy A, Alvi FS. Microjets-based active control of store trajectory in a supersonic cavity using a low-order model. AIAA *J* 2007;45(3):516–31 See also AIAA 2005-3097.
- [54] Pinney MA, Leugers JE. Experimental investigation of the impact of internal/external weapons carriage on a generic aircraft configuration. L-TR-96-3110, Final Report, Wright Laboratory, 1996.
- [55] Schmit RF, Schwartz DR, Kibens V, Raman G, Ross JA. High and low frequency actuation comparison for a weapons bay cavity. AIAA 2005-0795, January 2005.
- [56] Ukeiley LS, Ponton MK, Seiner JM, Jansen B. Suppression of pressure loads in resonating cavities through blowing. AIAA 2003-0181, January 2003.
- [57] Mongeau L, Franchek MA, Kook H. Control of interior pressure fluctuations due to flow over vehicle openings. In: Proceedings of the 1999 noise and vibration conference, May 1999, vol. 2. p. 1257–66.
- [58] Shaw L, McGrath S. Weapons bay acoustics—passive or active control. AIAA 96-1617, April 1996.
- [59] Cattafesta III LN, Garg S, Shukla D. The development of piezoelectric actuators for active flow control. AIAA *J* 2001;39(8):1562–8.
- [60] Cattafesta L, Mathew J, Kurdila A. Modeling and design of piezoelectric actuators for fluid flow control. *SAE 2000 Trans—J Aerosp (Sect 1)* 2001;109:1088–95.
- [61] Mathew J, Song Q, Sankar B, Sheplak M, Cattafesta L. Optimized design of piezoelectric flap actuators for active flow control. AIAA *J* 2006;44(12):2919–28.
- [62] Yokokawa Y, Fukunishi Y, Kikuchi S. Suppression of aero-acoustic noise by separation control using piezo-actuators. AIAA 2000-1931, June 2000.
- [63] Grove J, Birkbeck RM, Kreher JM. Acoustic and separation characteristics with bay leading edge blowing. AIAA 2000-1904, June 2000.
- [64] Grove J, Leugers J, Akroyd G. USAF/RAAF F-111 flight test with active separation control. AIAA 2003-0009, January 2003.
- [65] Smith BR, Jordan JK, Bender EE, Rizk SN, Shaw LL. Computational simulation of active control of cavity acoustics. AIAA 2000-1927, June 2000.
- [66] Williams DR, Cornelius D, Rowley CW. Supersonic cavity response to open-loop forcing. In: Proceedings of the first Berlin conference on active flow control, September 2006.
- [67] Williams DR, Fabris D, Morrow J. Experiments on controlling multiple acoustic modes in cavities. AIAA 2000-1903, June 2000.
- [68] Rowley CW, Williams DR. Control of forced and self-sustained oscillations in the flow past a cavity. AIAA 2003-0008, January 2003.
- [69] Raman G, Kibens V, Cain A, Lepicovsky J. Advanced actuator concepts for active aeroacoustic control. AIAA 2000-1930, June 2000.
- [70] Stanek MJ, Raman G, Kibens V, Ross JA, Odedra J, Peto JW. Suppression of cavity resonance using high frequency forcing—the characteristic signature of effective devices. AIAA 2001-2128, May 2001.
- [71] Chan S, Zhang X, Gabriel S. Attenuation of low-speed flow-induced cavity tones using plasma actuators. AIAA *J* 2007;45(7):1525–38.
- [72] Schlichting H. Boundary layer theory. 7th ed. New York: McGraw-Hill; 1979. p. 428–32.
- [73] Little J, Debiasi M, Caraballo E, Samimy M. Effects of open-loop and closed-loop control on subsonic cavity flows. *Phys Fluids* 2007;19.
- [74] Stanek MJ, Sinha R, Seiner J, Pierce B, Jones M. High frequency flow control—suppression of aero-optics in tactical directed energy beam propagation and the birth of a new model (part I). AIAA 2002-2272, May 2002.
- [75] Rizzetta DP, Visbal MR. Large-eddy simulation of supersonic cavity flowfield including flow control. AIAA 2002-2853, June 2002.
- [76] Kim K, Debiasi M, Schultz R, Serrani A, Samimy M. Dynamic compensator for a synthetic-jet-like compression driver actuator in closed-loop cavity flow control. AIAA 2007-880, January 2007.
- [77] Ziada S. Flow excited resonance of a confined shallow cavity in low mach number flow and its control. In: Proceedings of IMECE2002 ASME international mechanical engineering congress and exposition, November 2002.
- [78] Mongeau L, Kook H, Franchek MA. Active control of flow-induced cavity resonance. AIAA 98-2349, June 1998.
- [79] Kook H, Mongeau L, Franchek MA. Active control of pressure fluctuations due to flow over Helmholtz resonators. *J Sound Vibr* 2002;255(1):61–76.
- [80] Williams DR, Rowley C, Colonius T, Murray R, MacMartin D, Fabris D, et al. Model-based control of cavity oscillations—part 1: experiments. AIAA 2002-0971, January 2002.
- [81] Rowley CW, Williams DR, Colonius T, Murray RM, MacMartin D, Fabris D. Model-based control of cavity oscillations—part II: system identification and analysis. AIAA 2002-0972, January 2002.
- [82] Rowley CW, Williams DR, Colonius T, Murray RM, MacMynowski DG. Linear models for control of cavity flow oscillations. *J Fluid Mech* 2006;547:317–30.
- [83] Cabell RH, Kegerise MA, Cox DE, Gibbs GP. Experimental feedback control of flow-induced cavity tones. AIAA *J* 2006;44(8):1807–16 See also AIAA 2002-2497.

- [84] Kegerise MA, Cattafesta LN, Ha C-S. Adaptive identification and control of flow induced cavity oscillations. AIAA 2002-3158, June 2002.
- [85] Kegerise M, Cabell R, Cattafesta L. Real-time feedback control of flow-induced cavity tones. Part 1: fixed-gain control. *J Sound Vibr* 2007;307:906–23.
- [86] Kegerise M, Cabell R, Cattafesta L. Real-time feedback control of flow-induced cavity tones. Part 2: adaptive control. *J Sound Vibr* 2007;307:924–40.
- [87] Debiasi M, Samimy M. Logic-based active control of subsonic cavity flow resonance. AIAA J 2004;42(9):1901–9 See also AIAA 2003-4003.
- [88] Yan P, Debiasi M, Yuan X, Little J, Özbay H, Samimy M. Experimental study of linear closed-loop control of subsonic cavity flow. AIAA J 2006;44(5):929–38.
- [89] Samimy M, Debiasi M, Caraballo E, Serrani A, Yuan X, Little J, et al. Feedback control of subsonic cavity flows using reduced-order models. *J Fluid Mech* 2007;579:315–46.
- [90] Caraballo E, Little J, Debiasi M, Samimy M. Development and implementation of an experimental-based reduced-order model for feedback control of subsonic cavity flows. *J Fluids Eng* 2007;129(7):813–24.
- [91] Gallas Q, Holman R, Nishida T, Carroll B, Sheplak M, Cattafesta L. Lumped element modeling of piezoelectric-driven synthetic jet actuators. AIAA J 2003;41(2):240–7.
- [92] Shaw L. High speed application of active flow control for cavity acoustics. AIAA 2000-1926, June 2000.
- [93] Shaw L. Active flow control of weapons bay acoustics and vibration environments—current status. In: Proceedings of the 72nd shock and vibration symposium, November 2001.
- [94] Lou H, Alvi FS, Shih C, Choi J, Annaswamy A. Active control of supersonic impinging jets: Flowfield properties and closed-loop strategies. AIAA 2002-2728, June 2002.
- [95] Williams D, Morrow J. Adaptive control of multiple acoustic modes in cavities. AIAA 2001-2769, June 2001.
- [96] Ünalıms ÖH, Clemens NT, Dolling DS. Experimental study of shear layer/acoustics coupling in Mach 5 cavity flow. AIAA J 2001;39(2):242–52.
- [97] Garg S, Cattafesta III LN. Quantitative Schlieren measurements of coherent structures in a cavity shear layer. *Exp Fluids* 2001;30(2):123–34.
- [98] Kegerise MA. An experimental investigation of flow-induced cavity oscillations. PhD thesis, Syracuse University, Syracuse, NY, August 1999.
- [99] Smits AJ, Hayakawa K, Muck KC. Constant temperature hot-wire anemometer practice in supersonic flows. Part 1: the normal wire. *Exp Fluids* 1983;1(2):83–92.
- [100] Vakili AD, Wolfe R, Nagle T, Lambert E. Active control of cavity aeroacoustics in high speed flows. AIAA 95-0678, January 1995.
- [101] Kegerise MA, Spina EF, Cattafesta III LN. An experimental investigation of flow-induced cavity oscillations. AIAA Paper 99-3705, June 1999.
- [102] Kegerise MA, Spina EF, Garg S, Cattafesta III LN. Mode-switching and nonlinear effects in compressible flow over a cavity. *Phys Fluids* 2004;16(3):678–87 See also AIAA 98-2912.
- [103] Forestier N, Jacquin L, Geffroy P. The mixing layer over a deep cavity at high-subsonic speed. *J Fluid Mech* 2003;475:101–45.
- [104] Murray RC, Elliott GS. Characteristics of the compressible shear layer over a cavity. AIAA J 2001;39(5):846–56.
- [105] Meganathan AJ, Vakili AD. An experimental study of open cavity flows at low subsonic speeds. AIAA 2002-0280, January 2002.
- [106] Gharib M. Response of the cavity shear layer oscillations to external forcing. AIAA J 1987;25(1):43–7.
- [107] Micheau P, Chatellier L, Laumonier J, Gervais Y. Active control of a self-sustained pressure fluctuation due to flow over a cavity. AIAA 2004-2851, May 2004.
- [108] Haykin S. Adaptive filter theory. 4th ed. Upper Saddle River, NJ: Prentice-Hall, Inc.; 2002.
- [109] Kestens T, Nicoud F. Active control of unsteady flow over a rectangular cavity. AIAA 98-2348, June 1998.
- [110] Juang J-N. Applied system identification. Upper Saddle River, NJ: Prentice-Hall, Inc.; 1994.
- [111] Pillarisetti A, Cattafesta III, LN. Adaptive Identification of Fluid Dynamic Systems, AIAA 2001-2978, June 2001.
- [112] Holmes P, Lumley JL, Berkooz G. Turbulence, coherent structures, dynamic systems and symmetry. Cambridge: Cambridge University Press; 1996.
- [113] Rowley CW, Colonius T, Murray R. POD based models of self-sustained oscillations in the flow past an open cavity. AIAA 2000-1969, June 2000.
- [114] Rowley CW, Colonius T, Murray R. Dynamic models for control of cavity oscillations. AIAA 2001-2126, May 2001.
- [115] Ukeiley LS, Kannepalli C, Arunajatesan S, Sinha N. Low-dimensional description of variable density flows. AIAA 2001-0515, January 2001.
- [116] Rowley CW, Colonius T, Murray RM. Model reduction for compressible flows using POD and Galerkin projection. *Physica D* 2004;189(1–2):115–29.
- [117] Cain AB, Bower WW, McCotter F, Romer WW. Modeling and prediction of weapons bay acoustic amplitude and frequency. VEDA Inc.; February 1996.
- [118] Tam CKW, Block PJW. On the tones and pressure oscillations induced by flow over rectangular cavities. *J Fluid Mech* 1978;89(2):373–99.
- [119] Kerschen EJ, Tumin A. A theoretical model of cavity acoustic resonances based on edge scattering processes. AIAA 2003-0175, January 2003.
- [120] Alvarez JO, Kerschen EJ, Tumin A. A theoretical model for cavity acoustic resonances in subsonic flow. AIAA 2004-2845, May 2004.
- [121] Alvarez JO, Kerschen EJ. Influence of wind tunnel walls on cavity acoustic resonances. AIAA 2005-2804, May 2005.
- [122] Doyle JC, Francis BA, Tannenbaum AR. Feedback control theory. New York: Macmillan; 1992.
- [123] Kailath T. Linear systems. Englewood Cliffs, NJ: Prentice-Hall; 1980.
- [124] Kwakernaak H, Sivan R. Linear optimal control systems. New York: Wiley-Interscience; 1972.
- [125] Bélanger PR. Control engineering: a modern approach. Oxford: Oxford University Press; September 2005.
- [126] Skogestad S, Postlethwaite I. Multivariable feedback control analysis and design. 2nd ed. New York: Wiley-Interscience; November 2005.
- [127] Adrian RJ. On the role of conditional averages in turbulence theory. In: Proceedings of the fourth biennial symposium on turbulence in liquids. University of Missouri, Rolla, MO, September 1975.
- [128] Murray N, Ukeiley L. Estimation of the flowfield from surface pressure measurements in an open cavity. AIAA J 2003;41(5):969–72.
- [129] Rowley CW, Juttijudata V, Williams DR. Cavity flow control simulations and experiments. AIAA 2005-0292, January 2005.
- [130] Ukeiley L, Murray N, Song Q, Cattafesta L. Surface pressure based estimation for control. In: Morrison JF, Birch DM, Lavoie P, editors. IUTAM symposium on flow control and MEMS, September 2006, IUTAM Bookseries, vol. 7, 2008.
- [131] Rowley CW, Juttijudata V. Model-based control and estimation of cavity flow oscillations. In: Proceedings of the 44th IEEE conference on decision and control, December 2005.
- [132] Efe MÖ, Debiasi M, Yan P, Özbay H, Samimy M. Control of subsonic cavity flows by neural networks—analytical models and experimental validation. AIAA 2005-0294, January 2005.